Forschungszentrum Karlsruhe
Technik und Umwelt
Wissenschaftliche Berichte
FZKA 5813

ITER Coaxial Gyrotron Development

Final Report

M. Thumm, C. T. Iatrou, B. Piosczyk, O. Braz, G. Dammertz, S. Kern, M. Kuntze, A. Möbius

Institut für Technische Physik
Projekt Kernfusion
Association EURATOM-FZK

November 1996

Forschungszentrum Karlsruhe
Technik und Umwelt
Wissenschaftliche Berichte
FZKA 5813

ITER Coaxial Gyrotron Development

- Final Report -

M. Thumm*, C.T. Iatrou, B. Piosczyk, O. Braz*, G. Dammertz,
S. Kern*, M. Kuntze, A. Möbius

Institut für Technische Physik
Projekt Kernfusion
Association EURATOM-FZK

*also Universität Karlsruhe, Institut für Höchstfrequenztechnik und Elektronik,
Kaiserstr. 12, D-76128 Karlsruhe

Forschungszentrum Karlsruhe GmbH, Karlsruhe
1996

Forschungszentrum Karlsruhe GmbH
Postfach 3640, 76021 Karlsruhe

ISSN 0947-8620

ITER COAXIAL GYROTRON DEVELOPMENT

- Final Report -

Task No.: G 52 TT 03 94 - 08 - 03 FE
ID No.: T 24

Abstract:

A diode-type 4.5 MW coaxial-cavity-gyrotron electron gun having a central rod close to ground potential surrounded by the cathode ring (inverse magnetron injection gun, IMIG) has been designed and manufactured (U_c = 90 kV, beam current I_b = 50 A, velocity ratio $\alpha \approx 1.4$ and emitter current density j_e = 2.8 A/cm²). The emitter consists of LaB_6 and has an average radius of 56 mm. The properties of the electron beam have been measured with the method of retarding fields. The average value of α was found to be in good agreement with numerical predictions. The measured velocity spread $\delta\beta_{\perp rms} \cong 9\%$ is relatively high, but sufficiently low for reliable operation at the design parameters.

1.5 MW gyrotron oscillators with coaxial cavities designed for operation in the $TE_{28,16}$ and $TE_{31,17}$ modes at 140 and 165 GHz are under development and test. A maximum output power of 1.17 MW has been measured in the design mode at 140 GHz with an efficiency of 27.2 % (pulse duration 0.15 ms up to 0.5 ms). Single-mode operation has been found in a wide range of operating parameters. The experimental values agree very well with results of multimode calculations. Frequency step tuning has been performed successfully. Using a constant magnetic compression ratio, twenty modes have been excited in single-mode operation in the frequency range between 115.6 and 164.2 GHz. In particular, an output power of 0.9 MW has been measured in the $TE_{25,14}$ mode at 123.0 GHz and 1.16 MW in the $TE_{32,18}$ mode at 158.9 GHz.

The selection of the operating frequency and mode of the 165 GHz version is based on limitations imposed by the maximum magnetic field of the existing superconducting magnet and the use of the IMIG of the 140 GHz, $TE_{28,16}$ coaxial gyrotron. A maximum output power of 1.17 MW with an efficiency of 26.7 % has been measured in the design mode $TE_{31,17}$. Maximum efficiency of 28.2 % has been observed at an output power of 0.9 MW. Single-mode oscillation was also achieved in the $TE_{32,17}$ mode at 167.1 GHz, in the $TE_{33,17}$ mode at 169.4 GHz and in the $TE_{34,17}$ mode at 171.8 GHz with an output power of 1.02 MW, 0.63 MW and 0.33 MW, respectively. The power and efficiency decrease towards higher frequencies is due to the maximum achievable magnetic field of 6.6 T.

Optimization and design of a quasi-optical mode converter system compatible with the constraints of a coaxial-gyrotron dual-beam output concept for operation with two output windows is also presented. The two-step mode conversion sequences $TE_{-28,16}$ to $TE_{+76,2}$ to TEM_{00} at 140 GHz and $TE_{-31,17}$ to $TE_{+83,2}$ to TEM_{00} at 165 GHz have been investigated which both generate two narrowly-directed (60^o at the waveguide launcher) output wave beams. High conversion efficiences are expected (94 % and 92 %, respectively).

ITER KOAXIALGYROTRONENTWICKLUNG

- Schlußbericht -

Task No.: G 52 TT 03 94 - 08 - 03 FE
ID No.: T 24

Kurzfasssung:

Eine 4,5 MW Elektronenkanone (Diode) für Gyrotrons mit koaxialem Resonator, deren auf nahezu Erdpotential liegender zentraler Leiter vom Kathodenring umgeben ist (Inverse Magnetron Injection Gun, IMIG) wurde ausgelegt und hergestellt (U_c = 90 kV, I_b = 50 A, Geschwindigkeitsverhältnis $\alpha \approx 1{,}4$ und Stromdichte am Emitter j_e=2,8 A/cm²). Der Emitter besteht aus LaB_6 mit einem mittleren Radius von 56 mm. Die Eigenschaften des Elektronenstrahls wurden mittels der Gegenfeldmethode gemessen. Der mittlere Wert von α ist in guter Übereinstimmung mit numerischen Vorhersagen. Die gemessene Geschwindigkeitsstreuung $\delta\beta_{\perp rms} \cong 9$ % ist zwar relativ groß, aber immer noch klein genug, um einen verläßlichen Betrieb bei den Designparametern zu erlauben.

1,5 MW-Gyrotronoszillatoren mit koaxialem Resonator für die Moden $TE_{28,16}$ und $TE_{31,17}$ bei 140 bzw. 165 GHz wurden entwickelt und getestet. Eine maximale Ausgangsleistung von 1,17 MW bei einem Wirkungsgrad von 27,2 % wurde im Designmodus bei 140 GHz gemessen (Pulslänge 0,15 - 0,5 ms). In einem weiten Betriebsparameterbereich wurde Einmodenoszillation gefunden. Die experimentellen Ergebnisse stimmen gut mit Vielmodenrechnungen überein. Stufenweise Frequenzdurchstimmung wurde erfolgreich durchgeführt. Mit konstanter Magnetfeldkompression wurden im Frequenzbereich von 115,6 bis 164,2 GHz zwanzig Moden im Einmodenbetrieb angeregt. So wurden z.B. 0,9 MW im $TE_{25,14}$ bei 123,0 GHz und 1,16 MW im $TE_{32,18}$ bei 158,9 GHz gemessen.

Die Auswahl von Betriebsfrequenz und Betriebsmodus der 165 GHz-Version wird durch die obere Grenze des verfügbaren supraleitenden Magneten und durch den Gebrauch der IMIG des 140 GHz - $TE_{28,16}$ - Koaxialgyrotrons bestimmt. Eine maximale Ausgangsleistung von 1,17 MW bei einem Wirkungsgrad von 26,7 % wurde im Designmodus $TE_{31,17}$ gemessen. Der maximale Wirkungsgrad von 28,2 % wurde bei einer Ausgangsleistung von 0,9 MW beobachtet. Einmodenbetrieb wurde auch im $TE_{32,17}$ bei 167,1 GHz, im $TE_{33,17}$ bei 169,46 GHz und im $TE_{34,17}$-Modus bei 171,8 GHz erreicht und zwar mit Ausgangsleistungen von 1,02 MW, 0,63 MW bzw. 0,35 MW. Die Leistungs- und Wirkungsgradbegrenzung zu hohen Frequenzen hin ist durch das maximal erreichbare Magnetfeld von 6,6 T bedingt.

Optimierung und Auslegung eines quasioptischen Modenwandlersystems, das mit einem Zweistrahlauskoppelprinzip für koaxiale Gyrotrons mit zwei Ausgangsfenstern verträglich ist, werden auch vorgestellt. Die Zweistufen-Modenwandler-Sequenzen $TE_{-28,16}$ nach $TE_{+76,2}$ nach TEM_{00} bei 140 GHz und $TE_{-31,17}$ nach $TE_{+83,2}$ nach TEM_{00} bei 165 GHz, die beide jeweils zwei enggebündelte (60° an der Hohlleiterantenne) Ausgangsstrahlen erzeugen, wurden untersucht. Es werden hohe Konversionswirkungsgrade erwartet (94 % bzw. 92 %).

Contents

Summary

A diode type 4.5 MW electron gun having a central rod close to the ground potential surrounded by the cathode ring (inverse magnetron injection gun, IMIG) has been designed and manufactured according to the following design parameters: cathode voltage $U_c = 90$ kV, beam current $I_b = 50$ A, velocity ratio $\alpha \approx 1.4$ and emitter current density $j_e = 2.8$ A/cm^2. The emitter consists of LaB_6 and has an average radius of 56 mm. The properties of the electron beam, as the velocity ratio and the velocity spread, have been measured with the method of retarding fields. The average value of α was found to be in good agreement with numerical results. The measured velocity spread $\delta\beta_{\perp rms} \cong 9\%$ is relatively high but sufficient for reliable operation at the design parameters. In short pulse operation (≤ 0.3 msec) an electron beam current of above 50 A has been extracted at the design cathode voltage and no beam instabilities have been observed.

The design of the 1.5 MW, 140 GHz, $TE_{28,16}$ - coaxial cavity gyrotron is presented and results of experimental operation are given. In particular, a maximum output power of 1.17 MW has been measured in the design mode with an efficiency of 27.2% (pulse duration 0.15 msec up to 0.5 msec). Single mode operation has been found in a wide range of operating parameters. The experimental values agree very well with results of multimode calculations. The operating point with the design output power (1.5 MW) and efficiency (35%) is not accessible in the axial version probably because of enhanced mode competition due to window reflections. Frequency step tuning has been performed successfully. With a constant magnetic compression 20 modes have been excited in single mode operation in the frequency range between 115.6 and 164.2 GHz. In particular, an output power of 0.9 MW has been measured in the $TE_{25,14}$ mode at 123.0 GHz and 1.16 MW in the $TE_{32,18}$ mode at 158.9 GHz. At frequencies with strong window reflections the parameter range with stable operation is reduced significantly.

The design and experimental results of a coaxial cavity gyrotron operating in the $TE_{31,17}$ mode at 165 GHz are presented. The selection of the operating frequency and mode are based on limitations imposed by the maximum magnetic field of the existing super-conducting magnet at FZK and the use of the inverse magnetron injection gun of the 140 GHz, $TE_{28,16}$ coaxial gyrotron. In particular, a maximum output power of 1.17 MW with an efficiency of 26.7% has been measured in the design mode. A maximum efficiency of 28.2% has been observed at an output power of 0.9 MW. Modes with high window reflections are important competitors. Single mode oscillation was also achieved in the $TE_{32,17}$ mode at 167.1 GHz, in the $TE_{33,17}$ mode at 169.46 GHz and in the $TE_{34,17}$ mode at 171.8 GHz with an output power of 1.02 MW, 0.63 MW and 0.35 MW, respectively. The limitation towards higher frequencies are due to the maximum achievable magnetic field.

The optimization and design of a quasi-optical (q.o.) mode converter system compatible with the constraints of a coaxial gyrotron dual beam output concept for operation with two output windows are presented. The two-step mode conversion schemes $TE_{-28,16}$ to $TE_{+76,2}$ to TEM_{00} at 140 GHz and $TE_{-31,17}$ to $TE_{+83,2}$ to TEM_{00} at 165 GHz have been investigated which both generate two narrowly-directed (60° at the launcher) output wave beams. High conversion efficiences are expected (94% and 92%, respectively).

ITER Coaxial Gyrotron Development

Introduction

Conventional cylindrical-cavity gyrotrons are limited in output power and operating frequency (≈1 MW at 140 GHz) due to ohmic wall loading, mode competition, and limiting beam current. The problem of ohmic wall loading can be reduced by increasing the cavity diameter and using volume modes. The increased cavity diameter and the high operating frequency require operation in high-order modes, where the mode spectrum is dense and mode competition could prevent the gyrotron from stable operation. Furthermore, the use of volume modes, which do not load significantly the cavity walls, leads to lower limiting currents and reduced overall efficiency because of the increased voltage depression. These limiting factors can be considerably reduced with the use of coaxial cavities [1], which offer the possibility of selective influence of the diffractive quality factor of different modes, allowing operation in high-order volume modes with reduced mode competition problems. Furthermore, the presence of the inner conductor practically eliminates the restrictions of voltage depression and limiting current. Gyrotrons with coaxial cavities have the potential to generate, in cw operation, rf output powers in excess of 1 MW at frequencies above 140 GHz. In general, two methods are available in a coaxial cavity for an effective control of the diffractive Q-factor of different modes: (a) the use of a longitudinally corrugated tapered inner conductor [2], and (b) the use of a resistive inner conductor [3]. The first one seems preferable for high-power operation and it has been followed in the development of coaxial gyrotrons at FZK. A gyrotron with two different coaxial cavities designed for operation at frequencies of 140 GHz and 165 GHz with a rf output power in excess of 1 MW is under inverstigation at FZK.

Two configurations of the gyrotrons will be investigated in successive steps. First, the gyrotron will have an axial waveguide output with 100 mm diameter and will be operated at short pulses (0.3 ms), the maximum pulse length being limited by the heat load capability of the collector which is part of the output waveguide. Thereafter, as a step towards long-pulse operation, an improved tube with radial rf output will be investigated: the mm-wave power will be split into two beams and coupled out radially through two windows, and a single stage depressed collector will be used in order to enhance the total efficiency and to reduce the power loading at the collector surface.

The present ITER Coaxial Gyrotron Development Task T24 (EU) constists of the following subtasks:

Subtask 1: Measurement of the electron beam parameters and velocity spread of an inverse MIG gun.

Subtask 2: Test of the 140 GHz, 1.5 MW, $TE_{28,16}$ short pulse (0.3 ms) gyrotron with axial output.

Subtask 3: Experiments at 165 - 170 GHz frequency range with the $TE_{31,17}$ mode.

Subtask 4: Optimization and design of a q.o. mode converter system compatible with the coaxial gyrotron dual-beam output concept for operation with two output windows.

1. Subtask 1: Measurement of the Electron Beam Parameters and Velocity Spread of an Inverse Magnetron Injection Gun (IMIG) (Part of EU Base Program)

Summary

An inverse electron gun has been designed and manufactured for a 1.5 MW, 140 GHz coaxial gyrotron. During the design it was found that the axial shift of the gun with respect to the magnetic field may have an intolerable influence on the beam parameters. The accepted range of variation due to mechanical tolerances is small mainly because the gun is of the diode type and therefore has no independent adjustment for α. The chosen design is a compromise between the sensitivity against the axial shift and the velocity spread. The manufactured gun has been tested in a beam test device using scaled-down parameters. The average value of α agrees with the calculation. The measured velocity spread $\delta\beta_{\perp\mathrm{rms}} \cong 9\%$ is thought to be sufficiently small for reliable operation at the design parameters. In short pulse operation (≤ 0.3 msec) an electron beam current of above 50 A has been extracted at the design cathode voltage and no beam instabilities have been observed.

1.1 Measurement of the Electron Beam Parameters

A 4.5 MW electron gun has been designed in collaboration of IAP, Nizhny Novgorod and FZK Karlsruhe for a 1.5 MW, 140 GHz, $TE_{28,16}$ - gyrotron. The gyrotron was foreseen to be operated in an already existing superconducting (sc) magnet with a warm bore hole having a diameter of 275 mm. As a result of the magnetic field distribution the distance between the emitter and the center of the cavity is 344 mm.

The electron gun is of the diode type and has a central rod close to the ground potential surrounded by the cathode (inverse magnetron injection gun, IMIG). In Fig. 1 the manufactured gun is shown.

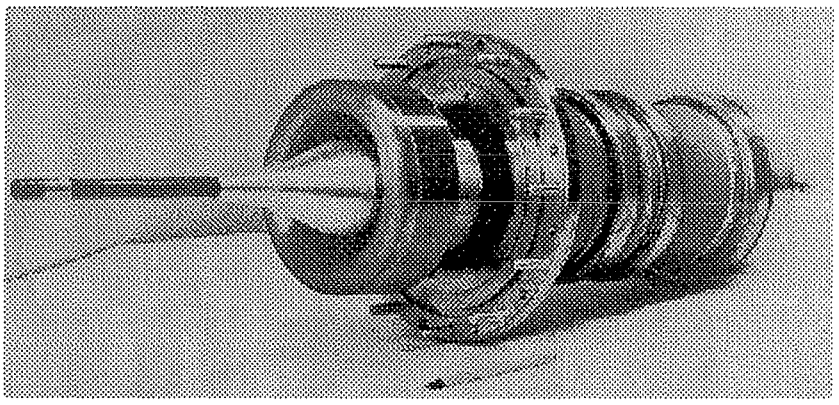

Fig. 1: Photograph of the 4.5 MW Inverse Magnetron Injection Gun.

The inner rod is electrically isolated but is held close to the ground potential. It is fixed and cooled from the gun side. It reaches up to about 25 cm above the resonator. The length is mainly determined by considerations of voltage depression. The part of the inner rod within and above the cavity can be easily replaced and it is not actively cooled. It can be radially adjusted during operation. The emitter material is out of LaB_6 and requires an operation temperature of about 1400° C . The main gun design parameters are summarized in Tab. 1. The numerical calculations have been done with the EPOSR-code as well as the EGUN-code. The maximum electric field is at the surface of the inner rod where the rod has its largest radius. The voltage depression at the resonator is only around 1 kV. In principal an arbitrary potential can be put on the inner rod in order to influence the potential drop along the beam path. The velocity ratio is $\alpha = \beta_\perp / \beta_\parallel$, where $\beta_\perp$ and $\beta_\parallel$ are the normalized electron transverse and parallel velocity averaged over the corresponding values of the single beamlets. The velocity spread $\delta\beta_{\perp max}$ is defined as $\delta\beta_{\perp max} = (\beta_{\perp max} - \beta_\perp) / \beta_\perp$ with $\beta_{\perp max}$ as the maximum transverse velocity achieved for a beamlet. The results achieved with the both codes agree very well. The corresponding rms-value of the transverse velocity spread is about $\delta\beta_{\perp rms} \approx 0.4\delta\beta_{\perp max}$. The values of the velocity ratio and velocity spread in bracketts have been calculated with EPOSR, the others with EGUN. The calculated velocity spread is relatively high at the design current. Geometries of the electrode shapes with lower spread have been found. However, they had to be rejected since they were accompanied by a strong sensitivity of the beam parameters to an axial displacement of the gun with respect to the position of the magnetic field. The chosen gun geometry shows nearly no effect for a displacement of the magnetic coils by ±4 mm relative to the gun. Also the sensitivity of the gun to a small displacement as well of the cathode and of the inner rod is sufficiently low.

Tab. 1: Design parameters of the inverse magnetron injection gun.

cathode voltage:	U_c	=	90 kV
beam current:	I_b	=	50 A
axial magnetic field at position of the emitter z_e:	B_e	=	0.207 T
axial magnetic field at position of the cavity $z_{c\,max}$:	B_0	=	5.543 T
average radius of the emitter:	R_e	=	56.0 mm
cathode tilt angle:	Φ_c	=	9.0°
axial width of the emitter:	Δz_e	=	5.0 mm
distance between center of emitter and cavity:	Δz_{ec}	=	343.5 mm
average beam radius at the cavity:	R_b	=	10.0 mm
beam thickness at the cavity:	ΔR_b	=	0.23 mm
maximum electric field within the gun:	E_c	=	7.0 kV/mm
maximum electric field at emitter surface:	E_e	=	3.8 kV/mm
calculated electron velocity ratio:	α	=	1.44 (1.35)
rms transverse electron velocity spread:	$\delta\beta_{\perp max}$	=	11.6 (9.1%)

After fabrication of the gun the beam parameters have been measured in a beam test device at scaled down parameters using the method of retarding fields. In collaborative experimental tests performed at IAP the electron beam parameters have been measured using the retarding field method with a down-scaling factor of $k = 15$. The experimentally measured relative transverse energy $t_\perp$ and velocity spread $\delta\beta_\perp$ as functions of the scaled beam current are plotted in Fig. 2 together with the theoretical predictions. The experimental value of $\delta\beta_\perp$ is evaluated by taking for the full width ($= 2\delta\beta_\perp$), the 90% and 10% value of the measured current distribution. The test device was operated in a magnetic field distribution different from the design system. The measured value of $t_\perp$ is in good agreement with the numerical calculations. The measured velocity distribution shows a spread of the transverse velocity $\delta\beta_{\perp\mathrm{rms}} \leq 9\%$. The discrepancy in $\delta\beta_\perp$ between the experimental and the maximum theoretical values are due to several effects such as initial thermal velocities, surface roughness etc. which are not considered in the calculations. In addition the high voltage performance and the emission capability have been tested with 20 μsec pulses.

The experimentally measured velocity spread is relatively high but is just sufficient for a reliable operation of the gun at the design velocity ratio α. In addition, mechanical and vacuum tests have been performed with positive results. The design considerations and the experimental results of the gun are described in detail in [4].

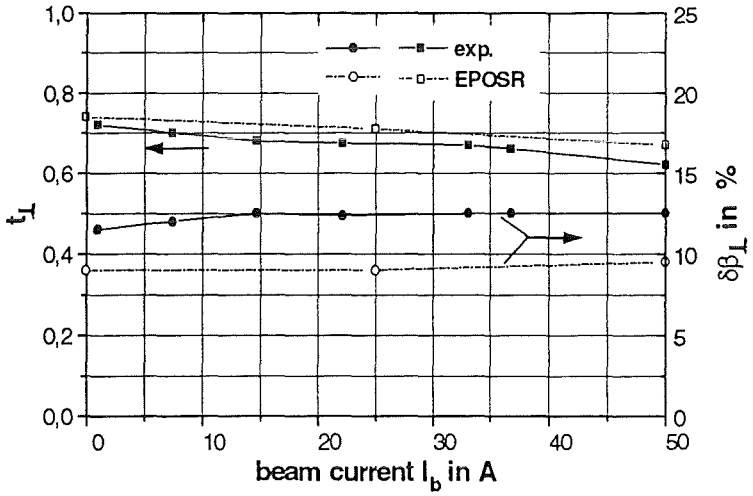

Fig. 2: Experimental values of relative transverse energy $t_\perp$ and velocity spread $\delta\beta_\perp$ for the coaxial $TE_{28,16}$ IMIG gun and comparison with theoretical predictions (for non-optimum magnetic field).

2. Subtask 2: Test of the Coaxial 140 GHz, 1.5 MW $TE_{28,16}$ - Short Pulse ($\leq$ 0.3 msec) Gyrotron with Axial RF - Output (Part of EU Base Program)

Summary

The design of the 1.5 MW, 140 GHz, $TE_{28,16}$ - coaxial cavity gyrotron is presented and results of experimental operation are given. In particular, a maximum output power of 1.17 MW has been measured in the design mode with an efficiency of 27% (pulse duration 0.15 msec up to 0.5 msec). Single mode operation has been found in a wide range of operating parameters. The experimental values agree very well with results of multimode calculations. The operating point with the design output power (1.5 MW) and efficiency (35%) is not accessible in the axial version probably because of enhanced mode competition due to window reflections. Frequency step tuning has been performed successfully. With a constant magnetic compression 20 modes have been excited in single mode operation in the frequency range between 115.6 and 164.2 GHz. In particular, an output power of 0.9 MW has been measured in the $TE_{25,14}$ mode at 123.0 GHz and 1.16 MW in the $TE_{32,18}$ mode at 158.9 GHz. At frequencies with strong window reflections the parameter range with stable operation is reduced significantly.

2.1 Introduction

Gyrotrons with coaxial cavities have the potential to generate in cw operation rf output powers in excess of 1 MW at frequencies above 140 GHz. On the contrary, gyrotrons with conventional cylindrical waveguide cavities with 1 MW output power at frequencies above 140 GHz are close to the technical limits mainly because of unacceptable high ohmic wall losses. In coaxial cavities the existence of the inner rod reduces the problem of mode competition and voltage depression thus allowing to use higher order modes than in cylindrical cavities resulting in lower ohmic losses. A gyrotron with coaxial cavities designed for operation at a frequency of 140 GHz with an rf-output power of 1.5 MW is under investigation at FZK Karlsruhe [5,6]. The development is planned to be performed in two steps.

In a first step, operated at short pulses ($\leq$ 0.3 ms) the gyrotron has an axial waveguide output with 100 mm diameter. The maximum pulse length was limited by the heat load capability of the collector, which is part of the output waveguide. In that version operating problems have been examined, the cavity design has been verified and further optimization with respect to single mode operation, efficiency and output mode purity have been done. For that the resonator and the inner rod have been designed for easy replacement.

In a second step a tube design relevant for cw operation with a radial rf output will be investigated. Especially because of the present power limit of rf output windows the mm-wave power will be split into two beams and coupled out radially through two windows. In addition, a single stage depressed collector will be used in order to enhance the total efficiency and to reduce the power loading at the collector surface.

The schematic layout of both versions is shown in Fig. 3. The main design parameters are summarized in Tab. 2. The main features of the gyrotron components are described in the following.

Tab. 2: Design parameters of the coaxial gyrotrons at 140 GHz ($TE_{28,16}$ - mode).

rf output power P_{out}	1.5 MW
cathode voltage U_c	90 kV
beam current I_b	50 A
velocity ratio α	1.35
cavity radius R_0	29.81 mm
beam radius R_b	10 mm
voltage depression ΔU	1.6 kV
peak wall loading (realistic) ρ_Ω	1.26 kW/cm^2

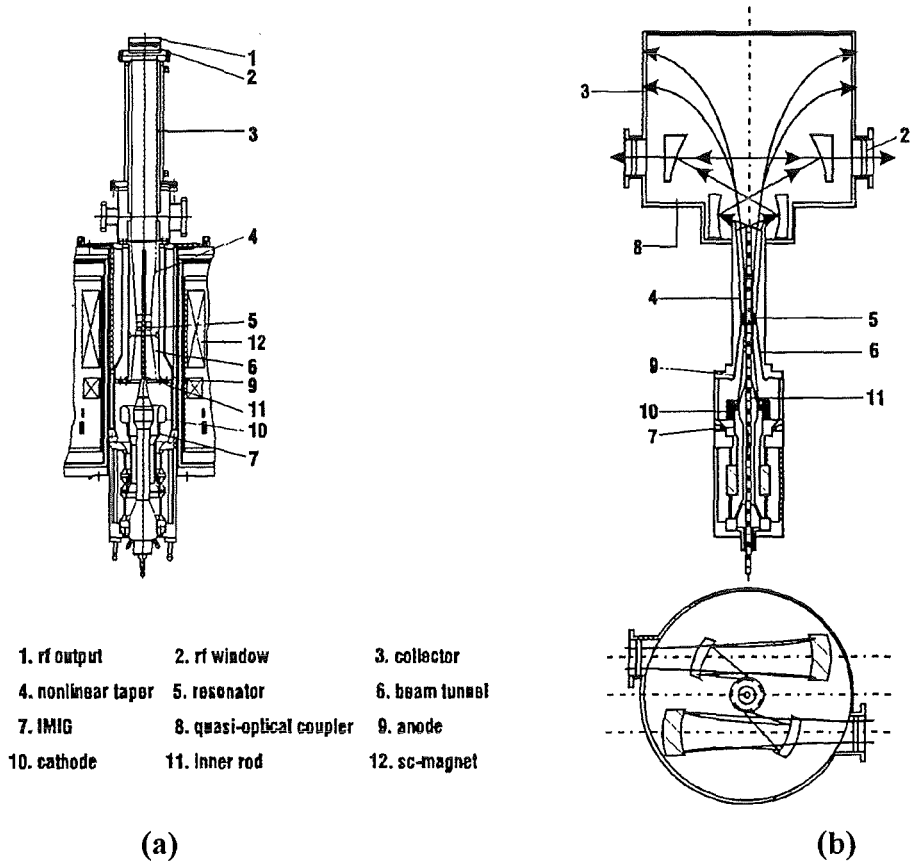

Fig. 3: Schematic layout of the coaxial cavity gyrotrons: (a) with axial rf-output, (b) with a dual-beam radial rf-output with two output windows.

2.2 The Superconducting Magnet and the Electron Gun

For the operation of the gyrotron tube an already existing superconducting magnet with a maximum magnetic field of 6.5 T and a warm bore hole having a diameter of 275 mm is used. In addition to the solenoidal coils the magnet has a set of dipol coils which enables a radial shift of the electron beam in the region of the cavity. With the help of these coils the alignment of the beam with respect to the inner rod can be proven. The electron gun is described in the foregoing chapter.

2.3 Cavity and Output Taper

The corotating $TE_{-28,16}$ mode with eigenvalue $\chi = 87.35$ was chosen as working mode for operation at 140 GHz. For the resonator (Fig. 4) a cavity with cylindrical outer wall and a radially tapered and corrugated inner rod is used. If the inner rod is tapered positively (radius decreases towards the collector), a positive/negative slope in the eigenvalue curve $\chi(C)$ of any mode will increase/decrease its diffractive quality factor [2]. The longitudinal impedance corrugation on the inner rod is introduced in order to avoid an increase of the quality factor of some competing modes. The influence of the corrugation on the eigenvalue is shown in Fig. 5. The corrugation consists of small longitudinal slots which imply no mode conversion because the period of the corrugation is small compared to $\lambda/2$, the free space half-wavelength. Appropriate tapering of the rod together with the impedance corrugation results in a significantly decreased diffractive quality factor of any mode which is influenced by the rod.

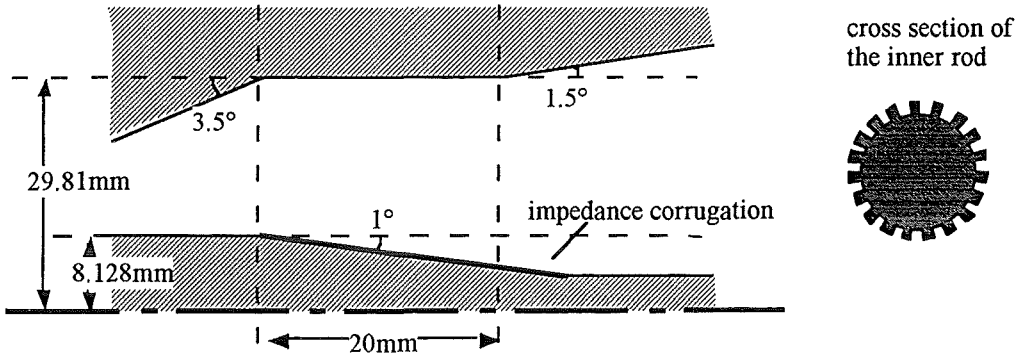

Fig. 4: Geometry of the $TE_{28,16}$ coaxial cavity with tapered and longitudinally corrugated inner rod.

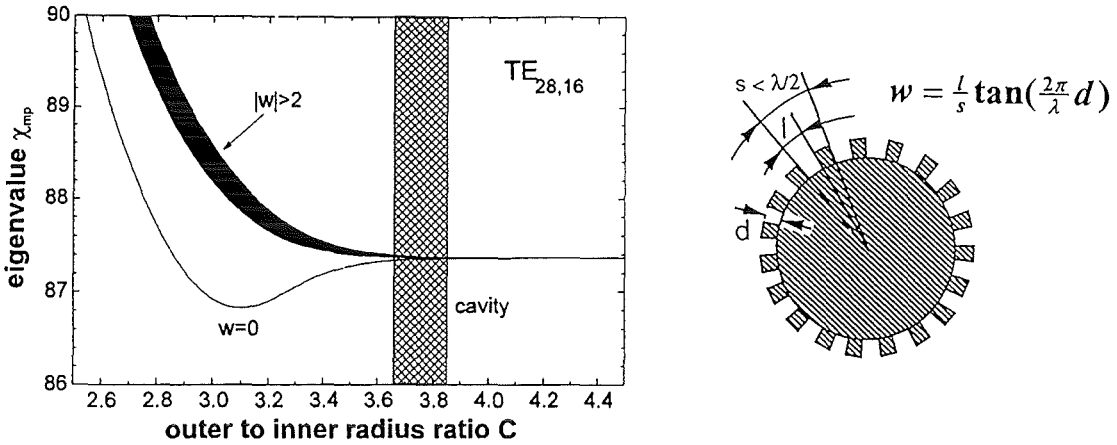

Fig. 5: Longitudinal corrugations of the inner rod and their influence on the eigenvalue.

The ratio C of the outer to inner radius in the cavity is such that the working mode is only slightly influenced by the inner rod. Then its Q-factor remains high while the diffractive quality factors of all other modes with higher radial index are reduced (Fig. 6) and consequently the starting currents are increased. Since modes with lower radial index couple significantly less to the electron beam, only modes with the same radial index as $TE_{27,16}$ and $TE_{29,16}$ remain as serious competitors. The azimuthal neighbours $TE_{27,16}$ and $TE_{29,16}$ have almost the same caustic radius with the operating mode therefore they are only slightly influenced by the inner conductor and hence their Q-factor is almost the same with that of the operating mode. This means that competition through the phase-amplitude mode interaction is still possible to take place. To suppress this kind of competition the azimuthal neighbours may be converted inside the cavity to modes which have a reduced Q-factor and couple out from the resonator. For the conversion the azimuthal neighbours must be degenerated with two other modes in the C-range of the cavity ($3.66 < C < 3.82$). The conversion to $TE_{+17,19}$ and $TE_{+15,20}$ can be achieved by introduction of longitudinal corrugation on the outer cavity wall (rippled wall converter) according to the formula:

$$R_c = R_{c,0} + \rho\cos(\Delta m\phi)$$

where $R_{c,0} = 29.8$ mm is the mean radius of the outer wall, $\rho = 0.066$ mm is the amplitude of corrugations and $\Delta m = 44$. The length of the converter is 20 mm, equal to the length of the cavity midsection. In this way stable single mode operation could be improved, if the stability of the operating mode is degraded due to competition against the azimuthal neighbours [7].

Self-consistent codes, which compute the electron beam - rf wave interaction, predicted an output power of 1.5 MW at 139.97 GHz in the $TE_{28,16}$ mode at a beam current of 42 A with an overall efficiency of 40%. The peak ohmic losses (ideal copper) are calculated to be 0.63 kW/cm^2 on the outer wall of the resonator and 0.07 kW/cm^2 on the inner conductor wall.

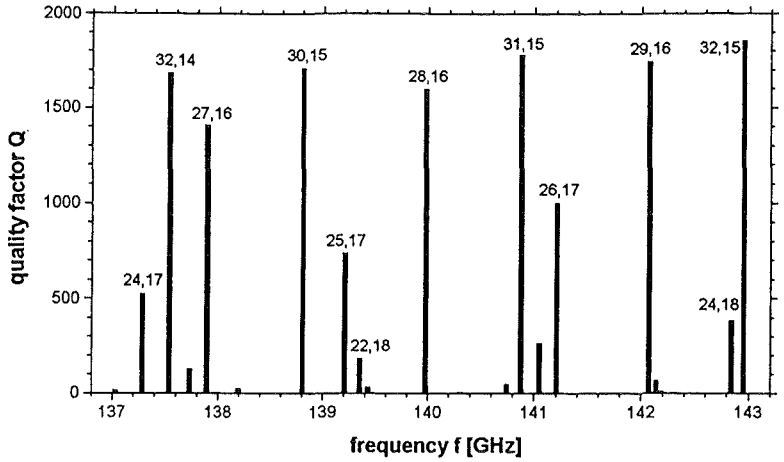

Fig. 6: Spectrum of the Q values for the coaxial cavity (modes with $m < 33$).

2.4 Collector and Output Window

In the first version the coaxial gyrotron will have an axial waveguide output (Fig. 3a) with a fused silica window of 100 mm diameter and a thickness of 4.61 mm corresponding to $9\lambda_e/2$ of the $TE_{28,16}$ mode at 140 GHz. The electron beam collector with the same diameter is a part of the output waveguide. The estimated electron beam power density at the collector surface is as high as 50 kW/cm^2 thus limiting the maximum allowable pulse length to about 300 μsec at the design beam parameters.

The second version with lateral dual beam output will have a single-stage depressed collector with an inner diameter of 300 mm allowing a maximum pulse length of several 10 msec. Two output windows out of fused silica are foreseen for use.

2.5 Quasi - Optical Mode Converter

For the operation with two rf output windows a q.o. mode converter system based on a two-step mode conversion scheme, $TE_{-28,16}$ to $TE_{+76,2}$ to TEM_{00}, which generates two narrowly-directed (60° at the launcher) output wave beams has been designed (Tab. 3 and Fig. 7). High conversion efficiencies are expected. The conversion of the cavity mode to the degenerate whispering gallery mode (WGM) is achieved by introduction of longitudinal corrugations in the output taper (1.5°) consisting of $\Delta m = 104$ slots according to the formula:

$$R_w = R_{w,0}(z) + \rho \cos(\Delta m \phi)$$

where $R_{w,0}(z)$ is the mean radius of the output waveguide wall, $\rho = 0.05$ mm is the amplitude of corrugations and $\Delta m = 104$. The q.o. converter will use an improved dimple double-beam launcher with $\Delta m_1 = 2$ and $\Delta m_2 = 6$ perturbations for longitudinal and azimuthal bunching of the two mm-wave beams. The dimensions of quasi-optical mode converter mirrors necessary for direct transformation of the $TE_{28,16}$ operating volume mode to a linearly polarized beam are too large for a dual beam output.

Tab. 3: Two-step mode conversion sequence compatible with the coaxial gyrotron dual beam output.

$TE_{-28,16}$	$TE_{+76,2}$	TEM_{00}
volume mode	whispering gallery mode	wave beam
degenerated modes longitudinal $\Delta m = 104$, waveguide mode converter		dual-beam output through two rf output windows

whispering gallery mode :

$$\text{TE76,2} \quad : \quad \varphi = 2\arccos\frac{m}{\chi_{mp}} = 59.14°$$

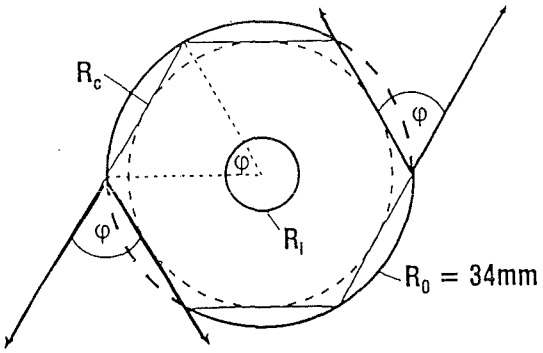

Caustic:

$$R_c = \frac{m}{\chi_{mp}} R_0 = 0.87 R_0 = 29.6mm$$

Fig. 7: Quasi-optical mode converter for coaxial gyrotron.

2.6 Present Status

2.6.1 Operation at 140 GHz with an Optimized Cavity with Corrugated and Tapered Inner Rod

At FZK the tube with an optimized cavity and corrugated and tapered inner rod has become first ready for measurements in August 1995. Soon after starting the experimental tests it turned out that unfortunately the current density was not uniform around the azimuth resulting in an approximately semicircular electron beam. This was because a part of the cathode filament was short-circuited causing an azimuthally non-uniform temperature distribution. A repair of the cathode filament became necessary.

After replacement of the filament the experiments started again mid of November 1995. During the measurements the following encouraging results have been achieved. The desired working mode $TE_{28,16}$ was found to work stable in a wide parameter range. This proves the suppression of possible competing modes by the impedance corrugated rod. A maximum rf-output power of 1.17 MW with an efficiency of 27.2% has been measured in the $TE_{28,16}$ mode in single mode operation at U_c = 86 kV, I_b = 50 A and B_0 = 5.63 T. The measured frequency of 139.96 GHz is close to the calculated value. The internal losses in the cavity, the output taper and the window are estimated to be 5.5%.

Figure 8 shows as an example the measured and the numerically calculated rf output power versus the beam voltage for a magnetic field of B_0 = 5.62 T and a beam current between 50 A and 52 A. The calculations have been performed with a multi-mode code using the operating parameters and the geometry of the cavity without any fitting and with an assumed velocity spread of 6%. As expected from the numerical calculations the azimuthal neighbours $TE_{29,16}$ at 142.02 GHz and $TE_{27,16}$ at 137.86 GHz, which are the remaining competitors, are limiting the stability region of the working mode in the U_c - B_0 parameter space. The experimentally observed regions with single and multi-mode oscillation are indicated at the top of Fig. 8. At a given magnetic field the $TE_{29,16}$ mode oscillates at a voltage below and the $TE_{27,16}$ above the oscillating range of the $TE_{28,16}$ mode. Single mode oscillation of the $TE_{28,16}$ mode is found within several kV of U_c. The regions of oscillations of the three measured modes agree well with the numerical predictions. Only the transition region is wider in the experiment than expected. According to calculations the rf power should rise up to U_c = 87 kV while the measured values reach a maximum around 84 kV and above about 86 kV the $TE_{27,16}$ mode is oscillating. In the region between U_c = 84 to 86 kV there is a small amount of the $TE_{27,16}$ mode present simultaneously with the $TE_{28,16}$ mode. This gives an explanation for the reduced efficiency and output power in that region. However, this multimoding is not predicted by the numerical calculations. The discrepancy is thought to be caused mainly by window reflections which support the competing $TE_{27,16}$

mode, since the rf window is optimized for 140 GHz and has a reflectivity of 10% at the frequency of the competitor. Another reason for the loss of single mode stability in higher voltages is overshooting of about 4% of the accelerating voltage (up to 3 - 4 kV) during a pulse. At the peak of the voltage the competing mode starts oscillations, and after the voltage dropped again these oscillations may remain. Both of these problems disappear in the tube with radial output. It has already been proven experimentally with conventional gyrotrons that window reflections do not influence the interaction in the cavity if a radial output is used. The overshooting of the used HV supply can be reduced by increasing the voltage rise time. This requires somewhat longer pulses and is foreseen in the tube with radial output. In consequence it is expected that the efficiency in that tube can be increased further.

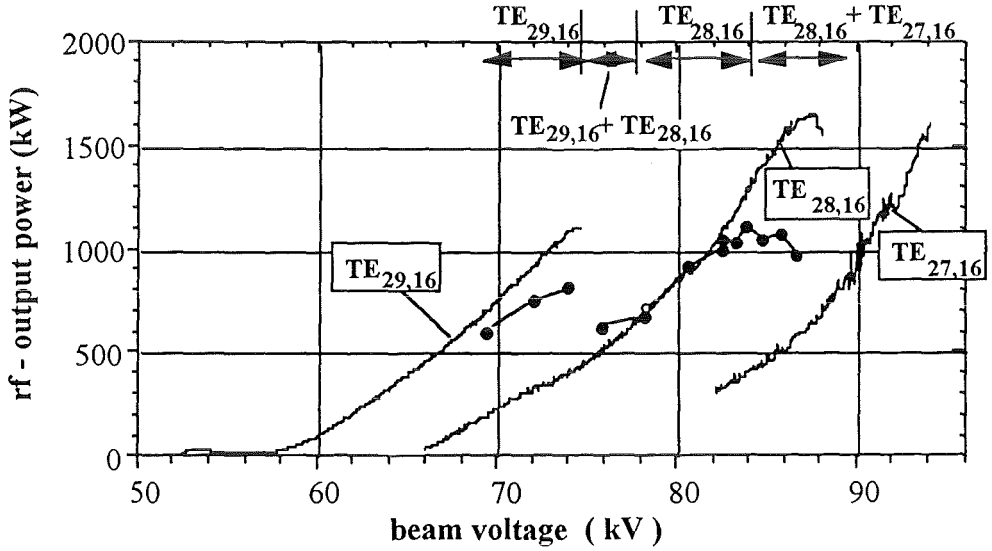

Fig. 8 : RF output power versus beam voltage. I_b = 50 - 52 A, B_0 = 5.62 T. Experimental results are given as points, with oscillating modes indicated at top. Solid lines are possible stable single mode operation points from multi mode calculations at the same parameters and taking into account 6% velocity spread.

The measurements have been performed with a pulse length of 150 μsec mainly because of the power loading at the collector wall. However, in single pulses the gyrotron has been operated up to 500 μsec. It turned out that the prealignment of the inner rod with respect to the cavity wall performed before mounting the tube was destroyed due to small mechanical deformation of the lower part of the gun on which the inner rod is fixed. The realignment of the inner rod with respect to the hollow electron beam became necessary and it was performed with the help of dipole coils which allow to move the electron beam within the cavity in radial direction. However, at the reported experiments there was no possibility to check the coaxiality of the inner rod with respect to the outer cavity wall when the tube was assembled. It has been estimated from previous measurements that the misalignment of the

inner rod and the cavity may be as high as about 0.5 mm. A possibility to check both the alignment of the outer cavity wall and of the inner rod with respect to the beam will be foreseen next.

To estimate the influence of the misalignment of the inner rod on the mode purity a series of measurements were done with defined misalignments. The distribution of rf power at the output was displayed by observing the thermal image on a target. It was found that a radial shift of the inner rod up to ±0.6 mm does not cause significant mode conversion. Apart from this, the waveguide mode purity was found to be disturbed, probably by inhomogenities due to the modular system after the cavity.

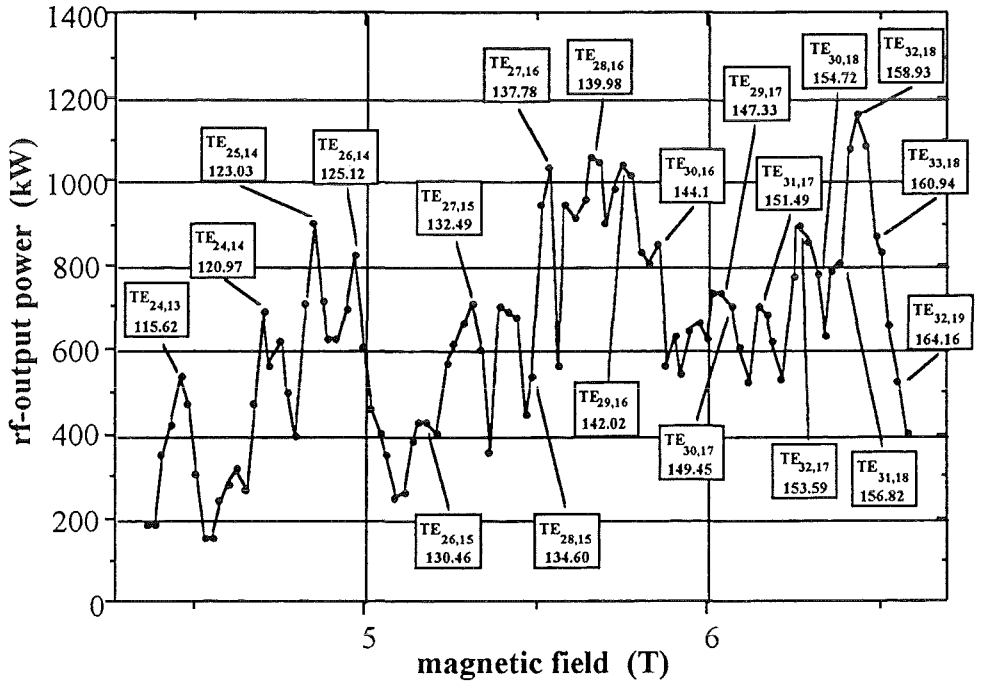

Fig. 9 : RF output power versus magnetic field. I_b = 50 - 52 A, beam radius R_b = 10 mm. Each point represents the stable single mode operation of the indicated mode.

The possibility of step tuning has been proven over a range from 115.6 GHz to 164.2 GHz using the same experimental configuration (Fig. 9). Frequency tuning was performed by changing the magnetic field with constant magnetic compression. Output powers around 1 MW and efficiencies above 25% have been achieved near frequencies where the window reflection is minimal (122 GHz, 140 GHz and 158 GHz). With high window reflections the gun could not be operated at the desired acceleration voltage because of beam instabilities, probably due to leakage of reflected and converted rf power towards the gun. However, these reflections will vanish in the tube with radial output. It is therefore expected that in the radial version any of the possible oscillating modes shown in Fig. 9 will have an output power and efficiency similar to modes at frequencies without window reflections. Table 4 gives some examples for excited modes. At frequencies above the design value the

maximum achievable velocity ratio decreases below the design value due to the need of higher magnetic field and the diode type of the used gun.

Tab. 4: Oscillating modes of the step tuning experiments at low window reflections.

P_{out} / MW	f / GHz	mode	B_0 / T	η_{tot} / %
0.9	123.03	$TE_{25,14}$	4.84	24.9
0.71	132.49	$TE_{27,15}$	5.31	17.6
1.17	139.98	$TE_{28,16}$	5.63	27.2
1.16	158.93	$TE_{32,18}$	6.43	26.2
0.83	160.94	$TE_{33,18}$	6.50	19.4

2.6.2 Gyrotron with a Dual - Beam Radial RF - Output

A gyrotron relevant for cw-operation with a dual transverse rf-beam output and a depressed collector is under construction. Components as output windows and the depressed collector are already ordered. The double beam launcher and the mirrors are under fabrication. The necessary modifications of the diagnostic equipment are under preparation.

2.7 Potential of Coaxial Cavity Gyrotrons

2.7.1 Estimated Limit for the Maximum Achievable CW Output Power

To estimate the maximum reachable output power of a coaxial gyrotron at a given frequency several technological limitations have to be considered. In the following investigations limitations due to the cavity and also due to the required electron gun are taken into account. The most important constraints are given in Tab. 5. Note that the maximum values of the wall loading refer to hot copper with realistic skin losses. Limitations related to the depressed collector have not been taken into account since they are not considered to be serious. Also the actually most important limitation of power due to the rf output window is not regarded here, this problem is discussed elsewhere. Since self-consistent calculations confirm that a single mode operating point is well described by the normalized variables formalism, the equations of this formalism are used to obtain expressions for output power and wall losses at a desired efficiency. This means also that stable single mode operation is assumed.

Tab. 5: Important limiting parameters in the estimation of achievable output power.

parameter	conservative limit	progressive limit
peak wall loading, ρ_Ω	≤ 2 kW/cm^2	≤ 3 kW/cm^2
emitter current density, j_e	≤ 3 A/cm^2	≤ 7 A/cm^2
electric field at emitter, E_e	≤ 70 kV/cm	≤ 70 kV/cm
beam current, I_b (not critical in coaxial cavity)	$\leq I_{lim} / 2$ (I_{lim}: limiting current)	
Fresnel parameter, C_F	≥ 1	≥ 0.7
emitter radius, R_e	≤ 55 mm	≤ 80 mm

Since the large number of constraints cannot be considered in a single analytic equation any more, a computer code was developed which optimizes the free parameters U_b, b (magnetic compression) and relative caustic radius m / χ of the operating mode for maximum output power under the given constraints. The efficiency is given, and the output power is obtained over the eigenvalue χ and with the normalized cavity length m as parameter. In Tab. 6 some results are given for the frequencies $f = 140$ GHz, 170 GHz and 270 GHz and for the two sets of limitations as given in Tab. 5. The efficiency is here around 35%, with $\alpha = 1.5$ and taking into account total losses of 15%, including ohmic losses in the cavity. The results are considered to be realistic, provided that single mode operation can be achieved. With the limits of stable single mode operation roughly estimated to be $\chi \leq 60$ for hollow waveguide, $\chi \leq 120$ for coaxial cavities with impedance corrugated rod and $\chi \leq 180$ with additional rippled wall converter, and with $10 \leq \mu \leq 25$ the achievable output powers are as summarized in Tab. 6.

Tab. 6: Achievable cw output power for conservative and progressive limiting parameters as given in Tab. 5.

frequency	geometry	conservative limits	progressive limits
140 GHz	hollow waveguide	1.1 MW	1.8 MW
	coaxial with impedance rod	2.0 MW	6.4 MW
	+ rippled wall converter		7.8 MW
170 GHz	hollow waveguide	0.7 MW	1.1 MW
	coaxial with impedance rod	1.3 MW	4.0 MW
	+ rippled wall converter		5.8 MW
270 GHz	hollow waveguide	0.2 MW	0.3 MW
	coaxial with impedance rod	0.5 MW	1.1 MW
	+ rippled wall converter		1.9 MW

2.7.2 Step Frequency Tunability

In gyrotron oscillators frequency tuning is performed by stepping through different working modes. With a coaxial cavity the possible operating modes within a small frequency range belong to the same radial series with constant radial index. The frequency difference between two of these modes is approximately $\Delta f = \pi f / (2\chi)$. In the actual experiment this stepsize is around 2-3 GHz.

It is well known that the oscillating frequency of a gyrotron is proportional to B_0 / γ. Fast frequency tuning can be achieved by changing γ, that means by changing the acceleration voltage. A usable region in voltage of $70\ \text{kV} \leq U_b \leq 130\ \text{kV}$ allows for fast frequency tuning (a few msecs) by ±5% of the center frequency. However, to keep the output power constant a triode gun with sophisticated control over the modulation voltage is required. Slow frequency tuning (some minutes) can be done over a much broader range by changing the magnetic field B_0. The accessible frequency range is here limited first by the interaction physics, and second by mode dependent structures in the coaxial cavity. If the interaction physics is again described by the normalized variables formalism a tuning range of ±15% is found using a diode gun with constant acceleration voltage. Output power and efficiency remain approximately constant over the tuning region, as was already experimentally proven. For a broader tuning region again a triode gun is required. The impedance corrugation works well within a frequency region of ±21%. If a rippled wall mode converter on the outer wall of the cavity is needed, roughly every second of the possible operating modes will be omitted. Therefore the frequency step will be doubled, $\Delta f = \pi f / \chi$, while the tuning bandwidth remains the same. In Tab. 7 the results are summarized and examples for the achievable tuning bandwidth are given.

Tab. 7: Tuning bandwidths.

method	properties	bandwidth	example
fast tuning (μsecs)	constant output power and efficiency only with triode gun	±5%	133 - 147 GHz
slow tuning with diode type gun (minutes)	constant output power efficiency roughly constant	±15%	120 - 160 GHz
slow tuning with triode type gun (minutes)	constant power and efficiency double stepsize with rippled wall converter	±21%	110 - 170 GHz

2.8 Further Development Needed

The goal of the development is to gain necessary results in order to be able to prepare a reliable technical layout of a coaxial gyrotron with an rf output power ≥1.5 MW operated at long pulses up to cw at a frequency ≥140 GHz. In addition, it is expected that out of the gained experience a reliable extrapolation towards the limit of the maximum achievable output power will be possible.

2.8.1 Gyrotron with Radial Dual - Beam Output and a Single -Stage Depressed Collector

The tube with the radial output is more relevant to a technical layout of a cw-gyrotron. In that stage a relatively robust gun technology is used and the components are designed for easy replacement. The disadvantages are the high operating temperature of the gun with moderate beam properties, a high outgassing rate and limited cooling capabilities. In that stage of experiments the following problems are foreseen to be examined:

- optimization of the dual-beam quasi-optical mode converter with an advanced dual-cut launcher and minimization of the rf-losses within the gyrotron tube
- investigation of the operation with depressed collector
- operation at longer pulse length (up to about 20 msec)

2.8.2 Design and Construction of an Improved Version of the Tube with Radial RF Output

In order to improve further the performance of the tube and the reliability of operation a new design of the gun and of other critical components had to be done taking into account the gained experience. In particular, for improving the vacuum and high voltage behavior the gun had to be redesigned and more advanced emitter materials like impregnated tungsten had to be used instead of LaB_6. By that the operating temperature will be reduced from 1400° C to about 1000° C. In addition, the alignment possibilities of the inner rod and the cavity with respect to the beam have to be improved.

3. Subtask 3: Experiments at 165 - 170 GHz Frequency Range with the $TE_{31,17}$ Mode

Summary

The development of a coaxial cavity gyrotron operating in $TE_{31,17}$ mode at 165 GHz is presented. The selection of the operating frequency and mode are based on the limitations imposed by the maximum magnetic field of the existing superconducting magnet at FZK, the use of the inverse magnetron injection gun of the 140 GHz - $TE_{28,16}$ coaxial gyrotron, and the possibility of transforming the cavity mode to a whispering gallery mode appropriate for the dual-beam quasi-optical output coupler and the two output windows, which are foreseen for the lateral-output version of the tube. The tube with axial output has been tested at FZK to deliver maximum power of 1.17 MW in the designed $TE_{31,17}$ mode with 26.7% efficiency at 164.98 GHz. Maximum efficiency of 28.2% was achieved at 0.9 MW output power. The design operating point with output power 1.36 MW and efficiency 36.7% is not accessible in the axial-output version of the tube because of enhanced mode competition due to window reflections and beam instabilities developed at high beam current and high electron velocity ratio. Power at higher frequencies was also detected; 1.02 MW at 167.14 GHz in $TE_{32,17}$ mode with 26.8% efficiency, 0.63 MW at 169.46 GHz in $TE_{33,17}$ mode with 18.0% efficiency, and 0.35 MW at 171.80 GHz in $TE_{34,17}$ mode with 13.3% efficiency.

3.1 Introduction

Conventional cylindrical-cavity gyrotrons have reached their power limits at high frequency operation ($\approx$ 1 MW at 140 GHz). To achieve output powers in excess of 1 MW at ITER relevant frequencies it is necessary to switch to coaxial-cavity geometry. The introduction of a tapered and longitudinally corrugated inner conductor in a cylindrical gyrotron cavity results in a significant modification of the diffractive quality factor spectrum, which allows operation in high-order volume modes with reduced ohmic wall loading and mode competition problems. In addition, voltage depression is drastically reduced resulting in high limiting current and thus to high beam current operation.

For performing the experiments, the cavity of the 140 GHz - $TE_{28,16}$ coaxial gyrotron of FZK has been replaced by a new coaxial cavity with tapered and corrugated inner conductor designed to oscillate at 165 GHz in the $TE_{31,17}$ mode. The rf output window has also been replaced by a new BN single-disk edge-cooled window with minimum reflections at the operating frequency. The rest of the tube (IMIG, beam tunnel, collector, etc) remained unchanged. As in the case of the 140 GHz - $TE_{28,16}$ tube, the 165 GHz - $TE_{31,17}$

coaxial gyrotron is first designed to operate with an axial output in short pulses because of the limited heat load capability of the collector, which is part of the 100 mm diameter output waveguide. In a next step towards a cw-relevant operation the tube will be operated with a lateral output using a dual-beam q.o. mode converter and a new single-stage depressed collector.

3.2 Selection of the Operating Mode and Cavity Design

There are two main limitations in the design of the coaxial gyrotron under description. The first is the use of the sc magnet existing at FZK, which can reach a maximum field around 6.5 T, and the second is the use of the inverse MIG of the 140 GHz - $TE_{28,16}$ coaxial gyrotron of FZK. This gun is designed to provide an electron beam of 50 A at 90 kV with an electron velocity ratio α of 1.44 at 5.54 T. Due to the first limitation of the sc magnet and the requirement of an operating frequency in the range 165 - 170 GHz, the acceleration voltage have to be reduced close to 75 kV, in order to increase the cyclotron frequency through a reduced relativistic mass factor γ. The reduction of the accelerating voltage from 90 to 75 kV and the increase of the cavity magnetic field from 5.6 to 6.5 T result in a considerably reduced value of the beam parameter α. The only available way to increase α is the increase of the magnetic compression through the reduction of the gun magnetic field. This means a smaller electron beam radius in the cavity, which in turn is limited by the diameter of the non-removable part of the inner conductor (16 mm), fixed to the IMIG.

Tab. 8: Beam radius R_b and velocity ratio α of possible operating mode families for the 165 GHz coaxial gyrotron.

azimuthal index m	beam radius R_b (mm)	beam α
29	8.82	1.8
30	9.12	1.4
31	9.41	1.1
32	9.71	0.8

Assuming a minimum acceptable beam radius in the resonator of 9 mm, only modes of the azimuthal families $m = 30$ (beam radius 9.12 mm) and $m = 31$ (beam radius 9.41 mm) were found to result in reasonable values of α, 1.40 and 1.10 respectively, according to EGUN calculations (Tab. 8). In view of the next version of the tube with a lateral output, the modes with azimuthal index $m = 30$ are excluded because non of them is degenerate with a WGM $TE_{m,2}$, in which the cavity mode should be transformed before the dual-beam output launcher. From the modes of the azimuthal family with $m = 31$ only the $TE_{31,17}$ (eigenvalue 94.62) is degenerate with a WGM mode, and in particular with the $TE_{83,2}$ (eigenvalue

94.69). The $TE_{31,17}$ mode was then selected to be the operating mode of the 165 GHz coaxial gyrotron [8].

A coaxial resonator has been designed, according to the design principles presented in [2] and [9], to oscillate in the $TE_{31,17}$ mode at 165 GHz, and it is shown in Fig. 10. The cut-off section of 22 mm length has an angle of 3.0° and it is connected to the 22 mm long cylindrical midsection with parabolic roundings of 4 mm for reduced mode conversion. Power transmission towards the gun is practically zero and mode purity of the downtaper is 99.3%. The linear part of the uptaper is 30 mm long with an angle of 1.5°. For the axial-output version of the tube a non-linear uptaper was designed and optimised to increase rapidly the diameter to 100 mm in a distance of 330 mm from the middle of the resonator with negligible mode conversion (mode purity 99.8%). The radius of the cylindrical part of the resonator is 27.38 mm (15 wavelengths). The inner conductor has a radius of 7.32 mm at the middle of the cylindrical part of the resonator, and it is downtapered by 1° towards the output. The selection of the inner-conductor radius is based on mode discrimination and wall loading considerations. The wall of this conductor is longitudinally corrugated with 72 rectangular grooves of 0.35 mm width and 0.38 mm depth, a value which is close to 0.21 times the free-space wavelength ensuring effective mode discrimination and reduced problems from possible mode competition from second cyclotron harmonic interaction [9].

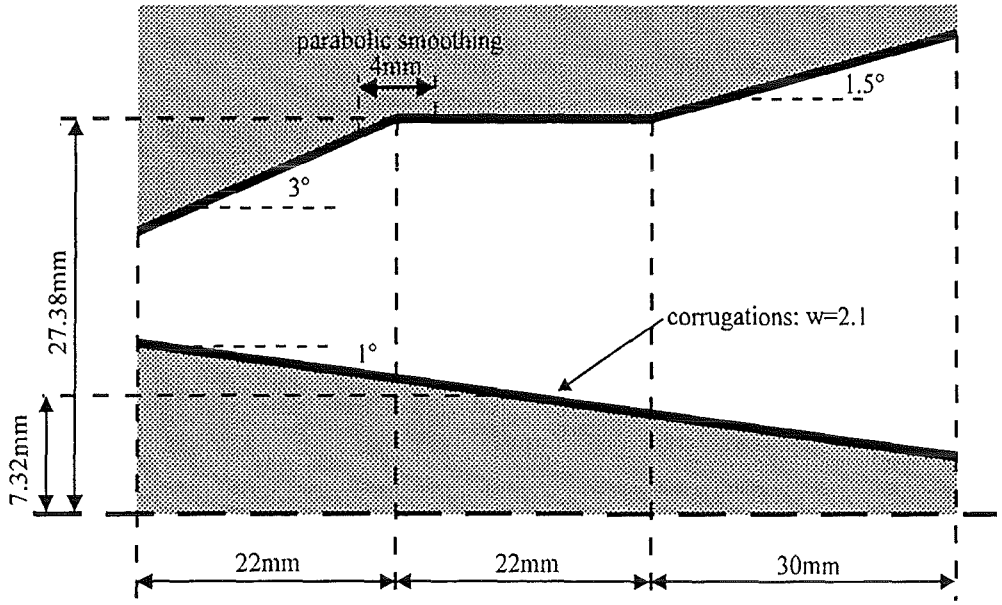

Fig. 10: Geometry of the 165 GHz - $TE_{31,17}$ coaxial resonator.

The normalized surface impedance w of the corrugated wall, given in [2]

$$w = \frac{l}{s}\tan\left(\chi_{mp}\frac{d}{R_o}\right)$$

takes the value of 2.1 at the middle of the resonator. Here, s is the period of corrugations, l is the width of the grooves, χ_{mp} is the mode eigenvalue, d is the depth of the corrugations, and R_o is the outer wall radius of the cylindrical part of the resonator. In Fig. 11, the mode eigenvalue χ_{mp} and the normalised impedance w are presented along the cavity axis. The normalised impedance varies within the cylindrical part of the resonator from 2.03 to 2.14, and along the total resonator from 1.93 to 2.31. The negative slope of the mode eigenvalue along the cylindrical part results in a slight decrease by 8% of the diffractive Q of the mode from the Q of this mode in an equivalent regular cylindrical resonator with length 22 mm.

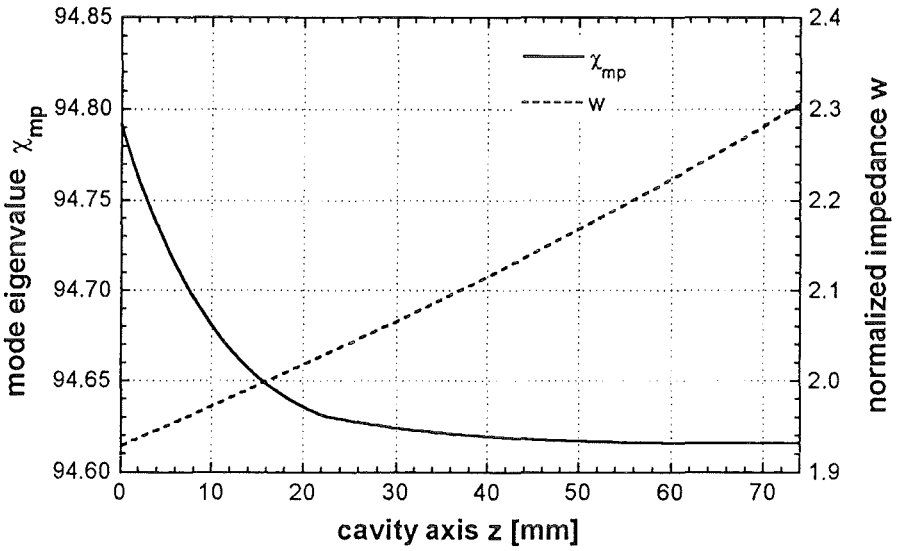

Fig. 11: Mode eigenvalue and normalised impedance of the $TE_{31,17}$ mode along the cavity axis.

The cold-cavity resonant frequency and diffractive Q of the $TE_{31,17}$ mode are 164.976 GHz and 3010. The relatively high diffractive Q is a result of the increased cavity length ($\approx$ 12 wavelengths), which is necessary to compensate the moderate accelerating voltage ($\approx$ 75 kV) and the low electron velocity ratio α ($\approx$ 1.0). The equivalent gaussian length L_g of the cold-cavity field profile is 24.5 mm, which corresponds to a normalised interaction length $\mu = \pi\alpha\beta_\perp L_g / \lambda$ equal to 16. The diffractive Q spectrum of the designed resonator is presented in Fig. 12. The frequency separation between the operating mode $TE_{31,17}$ and its azimuthal neighbours $TE_{30,17}$ and $TE_{32,17}$ is 2.268 GHz and 2.283 GHz, while their diffractive Q is 2685 and 3254, respectively.

The radius of the inner conductor was selected at 7.32 mm at the middle of the cavity midsection to provide effective mode selectivity by reducing the diffractive Q of the more volume modes as much as possible while keeping the ohmic loading of the inner conductor at low levels. The loading of the inner conductor increases rapidly with decreasing C due to higher magnetic field on the conductor surface [2], [9]. In Fig. 13 the peak ohmic loading is presented on both the outer cavity wall and the inner conductor surface along the cavity axis, assuming ideal cooper, rf power in the cavity 1.5 MW, diffractive Q 3010 for the $TE_{31,17}$ mode and a gaussian field profile along the cavity with equivalent length 24.5 mm.

The peak loading of the outer wall is found 1.15 kW/cm^2, and at the inner conductor is limited to 0.17 kW/cm^2.

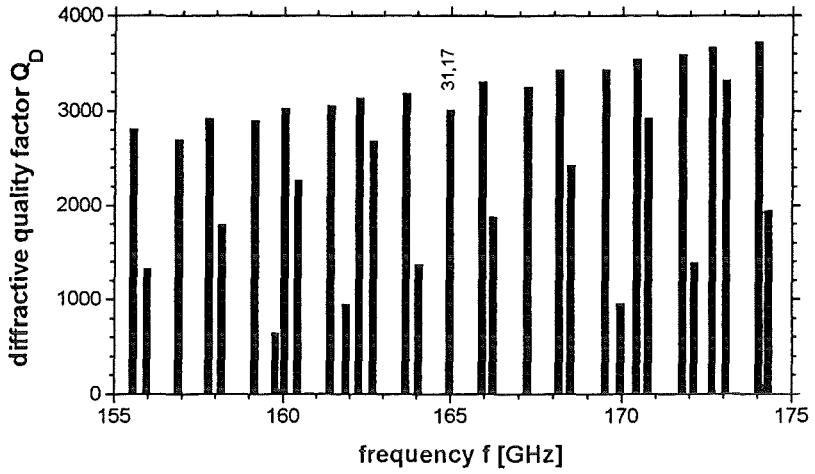

Fig. 12: Diffractive-Q spectrum of the 165 GHz - $TE_{31,17}$ mode coaxial cavity.

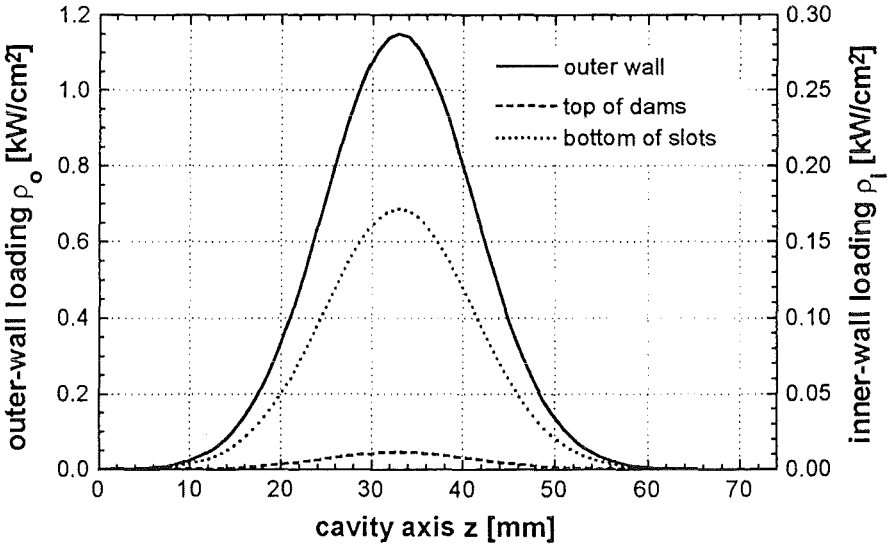

Fig. 13: Ohmic wall loading at 1.5 MW cavity power in the $TE_{31,17}$ mode (ideal cooper).

3.3 RF Output Window and Collector

The axial-output version of the 165 GHz - $TE_{31,17}$ mode coaxial gyrotron has a BN single disk edge cooled output window of 100 mm diameter with 3.967 mm thickness and 4.56 relative permittivity (measured values). The window was measured with a fundamental gaussian beam at 140 GHz and the extrapolated values showed minimum reflectivity of -32.8 dB at 164.8 GHz.

The collector is part of the output waveguide with 100 mm diameter. The estimated electron beam power density of the collector surface is close to 50 kW/cm^2 thus limiting the maximum allowable pulse length to about 300 μsec.

3.4 Interaction Calculations

The electron-guiding-center radius that corresponds to maximum coupling of the operating $TE_{-31,17}$ mode is at $R_b = 9.41$ mm. The mode spectrum of the product (quality factor) * (coupling coefficient) is presented in Fig. 14 for this beam radius.

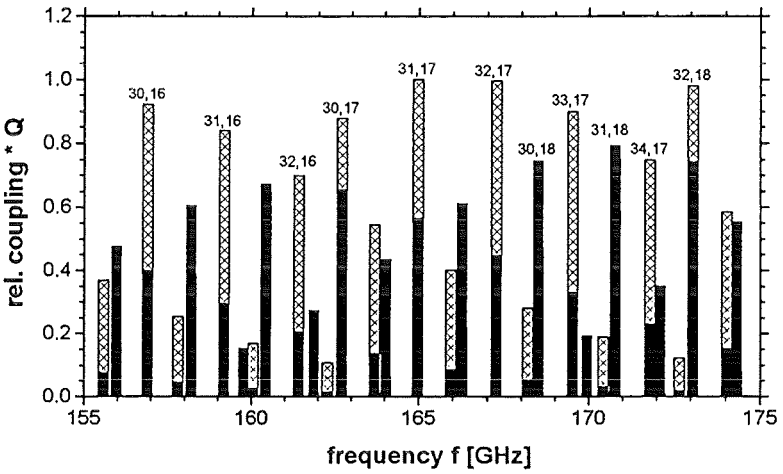

Fig. 14: Mode spectrum of the product (quality factor) * (coupling coefficient) for the 165 GHz coaxial gyrotron. Co-rotating modes are given with filled columns.

In Tab. 9 the most important competitors of the $TE_{-31,17}$ mode are given in terms of the relative product (diffractive Q) * (coupling coefficient).

Tab. 9: Competitors of the operating $TE_{-31,17}$ mode of the 165 GHz coaxial gyrotron.

Mode	Frequency (GHz)	Q*coupling	Mode	Frequency (GHz)	Q*coupling
-30,16	156.903	0.921	+29,18	166.266	0.611
+28,17	158.194	0.607	-32,17	167.260	0.997
-31,16	159.170	0.839	+30,18	168.515	0.747
-29,17	160.443	0.649	-33,17	169.527	0.898
+29,17	160.443	0.673	-31,18	170.782	0.755
-32,16	161.419	0.700	+31,18	170.782	0.792
-30,17	162.709	0.879	-34,17	171.793	0.748
+30,17	162.709	0.654	-32,18	173.066	0.979
-33,16	163.686	0.545	+32,18	173.066	0.742
-31,17	164.977	1	-35,17	174.043	0.585
+31,17	164.977	0.566	+30,19	174.339	0.553

The electron gun parameters computed by EGUN at the designed operating point (74 kV cathode voltage, 50 A beam current, and 6.48 T magnetic field) are given in Tab. 10. At different cathode voltage and cavity magnetic field the electron beam parameters are computed adiabatically.

Tab. 10: Parameters of the inverse magnetron injection gun

cathode voltage, U_c	74 kV
beam current, I_b	50 A
beam voltage, U_b	72.1 kV
cavity magnetic field, B_0	6.48 T
gun magnetic field, B_g	0.22 T
average emitter radius, R_e	56 mm
cathode tilt angle, ϕ_c	9°
axial width of the emitter, d_e	5 mm
emitter - cavity center distance, Δz_{ec}	343.5 mm
average cavity beam radius, R_b	9.5 mm
cavity beam thickness, ΔR_b	0.21 mm
maximum electric field at the gun, E_g	5.8 kV/mm
maximum electric field at the emitter, E_e	3.2 kV/mm
emitter current density, j_e	2.8 A/cm^2
electron velocity ratio, α	1.07
rms transverse velocity spread, $\delta\beta_\perp$	6%

The maximum achievable magnetic field of the sc magnet at FZK has been tested to be around 6.5 T. Since the magnet has been checked only twice to reach this value without quench, a study was performed for the maximum achievable output power in terms of the magnetic field, and the result is presented in Fig. 15. The magnetic field varies from 6.4 to 6.6 T and the cathode voltage U_c, resulting to maximum rf power, from 67 to 84 kV. The beam α is computed adiabatically to vary from 1.0 to 1.18, the beam radius is at 9.50 mm and the beam current is kept constant at 50 A. The output power, which is computed from the rf power generated in the cavity reduced by 7% due to assumed ohmic losses in the cavity and the output waveguide, reaches the value of 1.55 MW at 6.58 T with output efficiency of 36%. At 6.48 T, which will be the design value, the output power is 1.48 MW with efficiency 38.8%. These points have been computed using a stationary single-mode code and they have not been checked in terms of stability. In any case they give a sense of the benefits expected from an increased magnetic field.

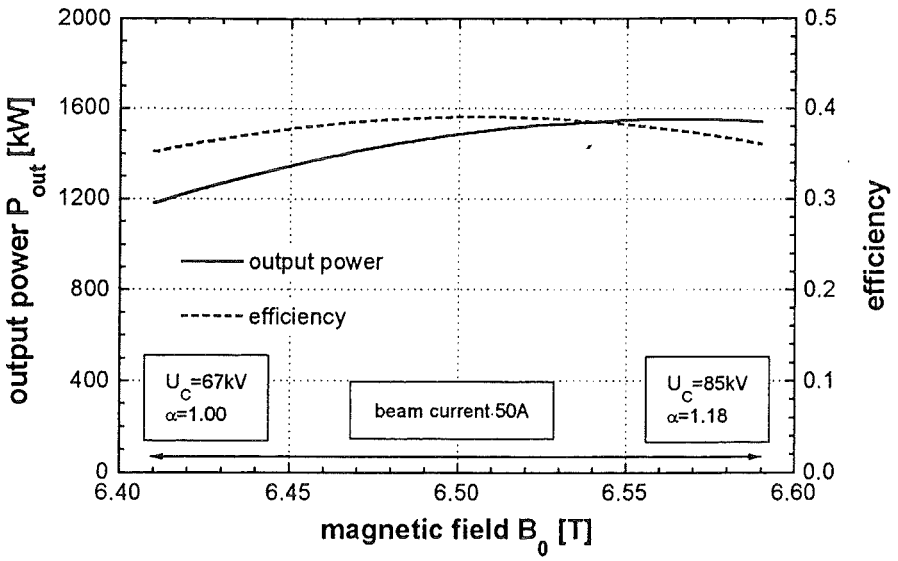

Fig. 15: Output power and total efficiency of the $TE_{31,17}$ mode versus the magnetic field. The cathode voltage is optimized for maximum power. The beam α follows adiabatically the cathode voltage and the magnetic field. The beam current is fixed at 50 A.

The output power and efficiency have been also computed varying the beam current from 40 to 60 A at 6.48 T magnetic field and 74 kV cathode voltage and they are presented in Fig. 16. The beam α is kept constant at 1.07. The results are from the stationary single-mode code and no stability of oscillations has been considered. At 40 A the output power is 1.08 MW and at 60 A it reaches 1.56 MW. The maximum efficiency is 38.4% at 44 A.

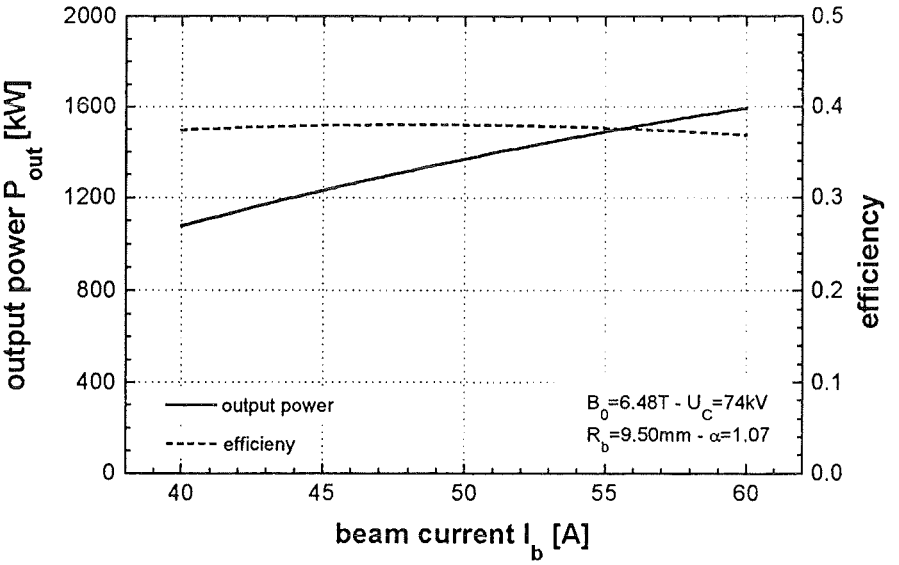

Fig. 16: Output power and total efficiency in the $TE_{31,17}$ mode versus the beam current.

The influence of velocity spread was also studied and the results are presented in Fig. 17. Here all the parameters are fixed at the design values, that is: magnetic field 6.48 T, cathode voltage 74 kV, beam current 50 A, beam radius 9.50 mm, and beam α 1.07. A 10% rms transverse velocity spread reduces the output power by 60 kW and the efficiency by 1.5%.

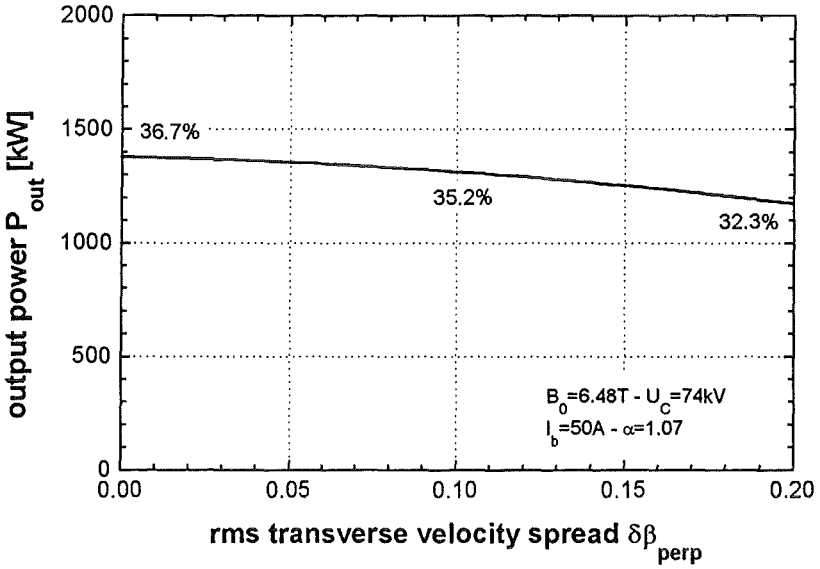

Fig. 17: Output power reduction due to transverse electron velocity spread at the designed operating point of the $TE_{31,17}$ mode.

The starting current of the operating mode and its competitors was computed in terms of the beam voltage (beam voltage in the cavity after voltage depression) and it is presented in Fig. 18. Here the magnetic field is constant at 6.48 T while the beam α follows adiabatically the beam voltage. The evolution of the beam current is also shown in Fig. 18. The figure is useful to determine the oscillating-mode sequence during the startup of the tube, where the cathode voltage and beam current rise from zero to their operating values. According to this figure, the first mode to be excited during the startup is the $TE_{33,17}$ at a beam voltage close to 30 kV, which will be replaced by the $TE_{32,17}$ close to 52 kV. The operating mode $TE_{31,17}$ is expected to start oscillations at 62 kV beam voltage ($\approx$ 64 kV cathode voltage) and to keep oscillating stably up to 72 or 74 kV beam voltage. The hard-excitation region of the operating mode starts close to 68 kV beam voltage.

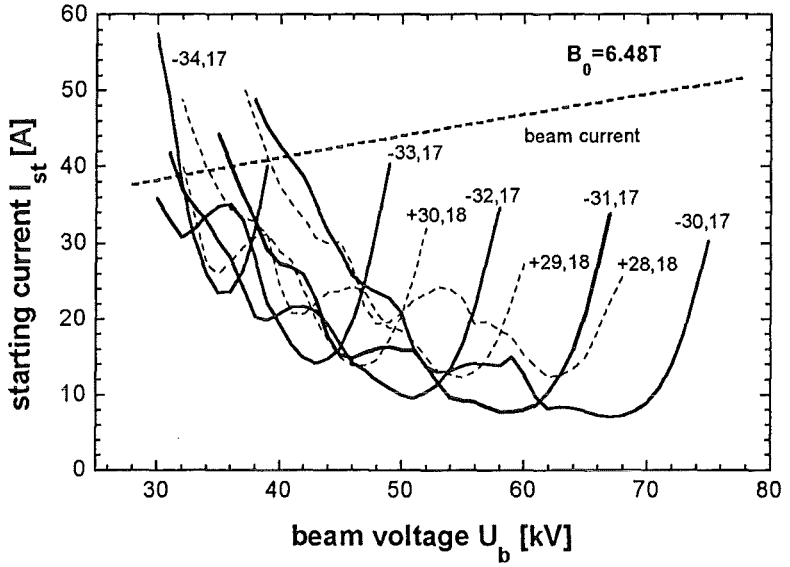

Fig. 18: Starting current of the operating mode and its competitors versus the beam voltage.

The output power and efficiency achieved in each mode during the rise of the cathode voltage has been computed at the designed magnetic field of 6.48 T and it is presented in Figs 19. The velocity ratio α follows adiabatically the cathode voltage and it reaches the value of 1.07 at 74 kV cathode voltage and 50 A beam current. A time-dependent multi-mode code has been used and all the points of the plot have been checked in terms of stability. The mode $TE_{33,17}$ is first excited at 34 kV and it reaches stably 0.39 MW at 50.7 kV with 17.8% total efficiency. Then the next azimuthal neighbour $TE_{32,17}$ starts oscillations and it reaches 0.83 MW at 62.3 kV with 28.5% efficiency. At higher voltages it is suppressed by the operating mode $TE_{31,17}$, which reaches stably an output power of 1.34 MW at cathode voltage 74 kV with efficiency 36.2%. At even higher voltages the operating mode looses oscillations suppressed by its neighbour $TE_{30,17}$. The mode stability has been checked using the oscillating mode and two pairs of next and over-next azimuthal neighbour modes and leaving the beam voltage constant for a time interval of 200 nsec. The oscillating region of the $TE_{31,17}$ mode has been found, using the stationary single-mode code, to extend up to 75.5 kV cathode voltage. For cathode voltage from 74 to 75.5 kV multimode operation was found with power in $TE_{31,17}$ and $TE_{30,17}$ modes. The dependence of beam current and electron velocity ratio on the cathode voltage assumed during the startup is presented in Fig. 20.

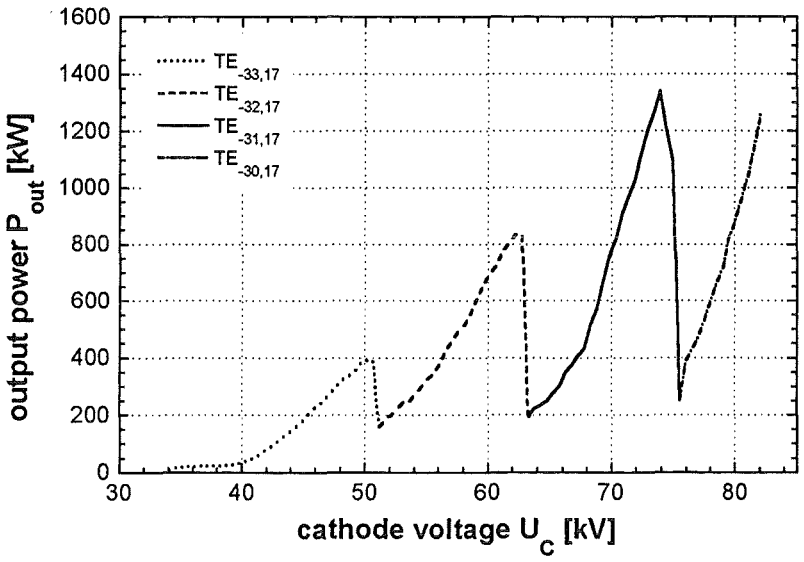

Fig. 19a: Output power in different modes excited during the startup versus the cathode voltage at $B_0 = 6.48$ T, $R_b = 9.50$ mm, $\delta\beta_{\perp,rms} = 6\%$.

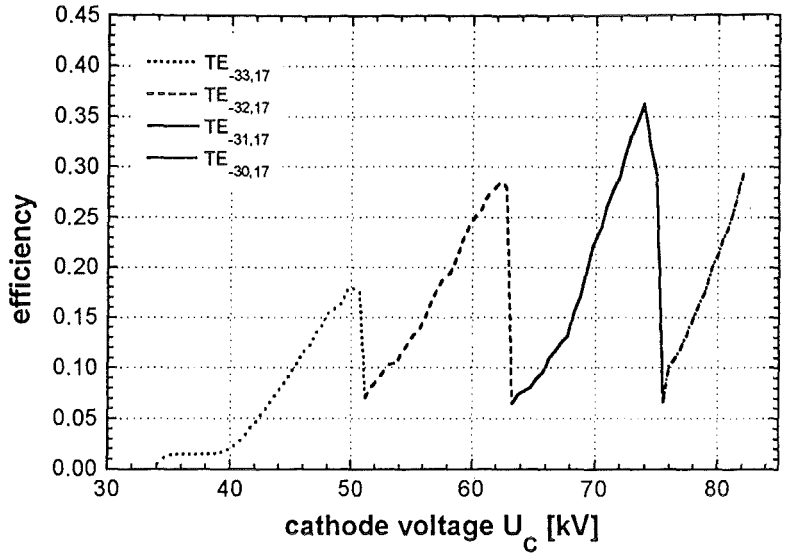

Fig. 19b: Total efficiency in different modes excited during the startup versus the cathode voltage at $B_0 = 6.48$ T, $R_b = 9.50$ mm, and $\delta\beta_{\perp,\mathrm{rms}} = 6\%$.

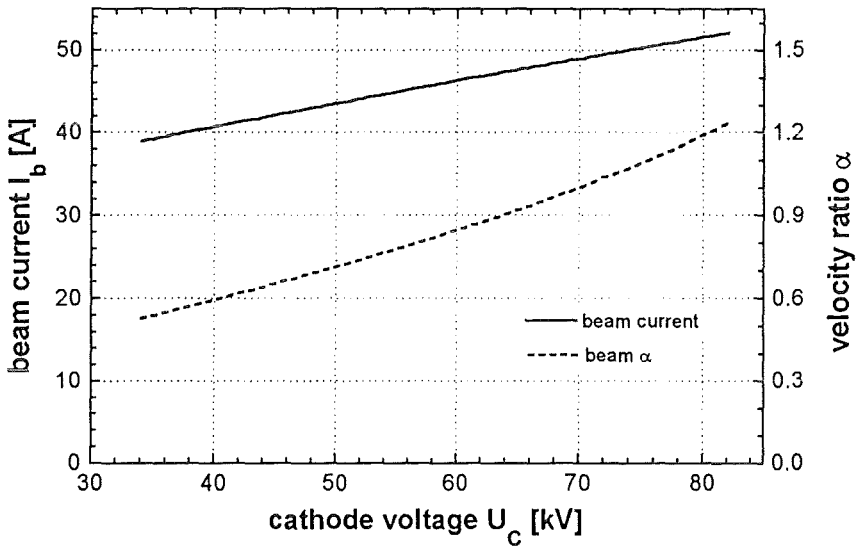

Fig. 20: Beam current and electron velocity ratio versus the cathode voltage at $B_0 = 6.48$ T, $R_b = 9.50$ mm and $\delta\beta_{\perp,\mathrm{rms}} = 6\%$.

In Fig. 21 the stability region in the B_0 - U_b plane is presented for the operating mode and its high-frequency azimuthal neighbours. Here the iso-power curves refer to rf power, that is microwave power generated by the beam in the cavity. The output power is assumed to be 7% lower due to overall ohmic losses. An output power in excess of 1 MW seems to be reachable in a wide range of magnetic field and beam voltage values.

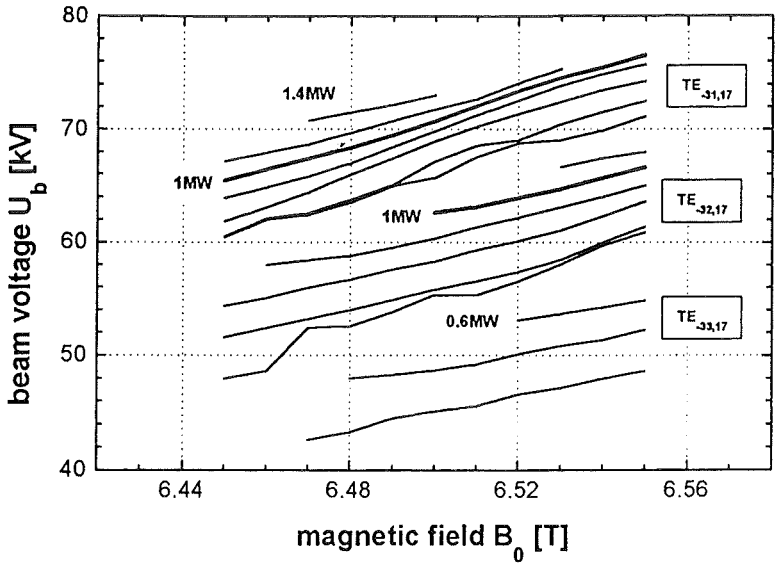

Fig. 21: Stability region of the operating mode and its high-frequency azimuthal neighbours in the B_0 - U_b plane.

The self-consistent results of the stable oscillations at the operating point are summarized in Tab. 11.

Tab. 11: Self-consistent results at the designed operating point.

operating mode	$TE_{31,17}$
magnetic field, B_0	6.48 T
cathode voltage, U_c	74 kV
beam voltage, U_b	72.1 kV
beam current, I_b	50 A
electron velocity ratio, α	1.07
frequency, f	164.98 GHz
rf power w/o losses, P_{rf}	1.46 MW
electronic efficiency, η_{elec}	40.6%
output power, P_{out}	1.36 MW
total efficiency, η_{tot}	36.7%
cavity wall losses, P_Ω	29 kW
peak wall loading on outer wall, ρ_o	0.95 kW/cm^2
peak wall loading on inner wall, ρ_i	0.14 kW/cm^2
diffractive quality factor, Q_D	2956
ohmic quality factor, Q_Ω	147386
equivalent gaussian field length, L_g	24.2 mm
normalized field length, μ	15.74
normalized detuning, Δ	0.59
normalized field amplitude, F	0.16

3.5 Experimental Results and Comparison with Numerical Simulations

The 165 GHz - $TE_{31,17}$ mode coaxial gyrotron has been tested in pulsed operation with pulse duration 150 μsec and repetition rate 1 Hz. The two gun-coils that can be energized separately allow some limited control on the beam pitch factor, although the inverse MIG used in the experiment is a diode type gun. Energizing the first gun-coil (ES1), the one below the cathode, results in a relatively high beam α, but in a high velocity spread as well. That was the first choice in the experiment. At the begining of the experiment stable single-mode operation of the device was almost impossible or limited in power ($\approx$ 0.5 MW) and restricted to a narrow range of parameters, due to unusally high ripples of the cathode voltage ($\pm$ 5-10 kV) and the beam current ($\pm$ 10-15 A), especially at the begining of the pulse. To stabilize the voltage pulse the voltage regulator tube was put off the circuit and the gyrotron was directly open to the high voltage. A reasonably stable cathode voltage and beam current pulse was then obtained and the tube operation in terms of stability and monomode operation was considerably improved.

The experimentally achieved maximum output power in the $TE_{31,17}$ mode and the corresponding total efficiency are presented in Figs 22 in terms of the beam current. All the experimental data, except the last two at high beam current, correspond to magnetic field 6.55 T and beam radius 9.62 mm. The cathode voltage was optimized to achieve maximum output power and it was in the range from 75 to 76.5 kV. For the last two experimental points, at 50.1 and 52 A, the magnetic field was 6.61 T and the beam radius 9.57 mm. The cathode voltage was 83.4 and 84.8 kV, respectively. The reference point for computing adiabatically the beam α was the following: at 6.55 T magnetic field, 9.62 mm beam radius in the cavity, 77 kV cathode voltage and 40 A beam current, the EGUN-code computed a beam α equal to 1.0. In Figs 22 the results of the self-consistent single-mode code are presented at three different cathode voltages; the experimentally measured cathode voltage, and at plus/minus 1 kV from this value. The rms transverse velocity spread used in the simulations is the one predicted from EGUN, equal to 7%. The output power was computed in the simulations from the rf power generated in the cavity (without ohmic losses) reduced by 7% due to ohmic losses in the cavity, the output waveguide, and the window. The experimental results are well within the three theoretical curves. The range of $\pm$1 kV is within the measuring uncertainty of the cathode voltage.

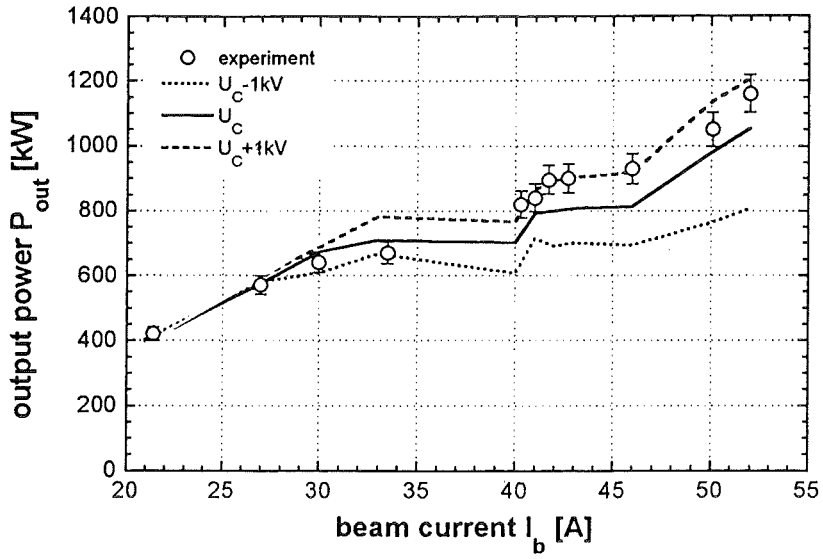

Fig. 22a: Maximum experimental output power and numerically computed output power in $TE_{31,17}$ mode versus the beam current.

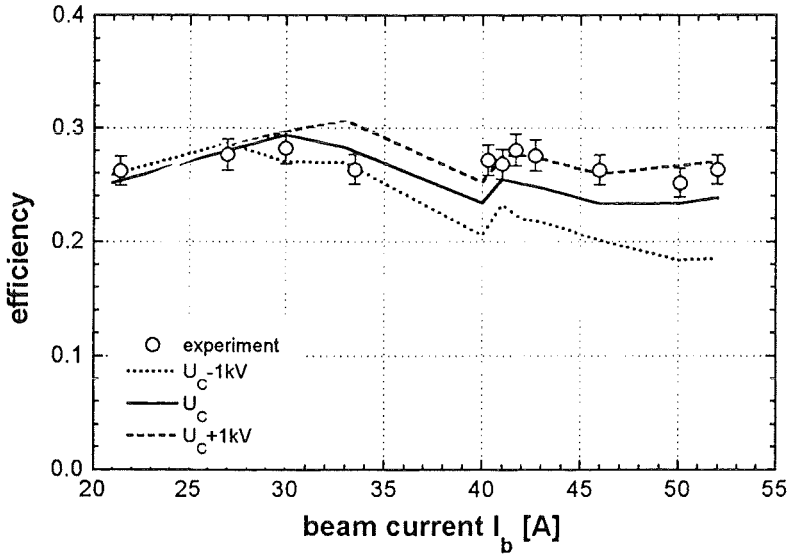

Fig. 22b: Total efficiency versus beam current corresponding to output power given in Fig. 22a.

Although there is a very good agreement between the experimental and numerical results presented in Figs 22, it must be mentioned here that the experimentally obtained output power is the maximum possible while the computed output power is not the maximum, but simply the output power computed at the experimental parameters. At a given beam current it is possible in the simulations to increase further the cathode voltage and to obtain even higher power. This was impossible in the experiment. In Fig. 23 the maximum output power (experimental and numerical) it is presented. The experimental data are the same as in Fig. 22a. The theoretical curves were computed from two self-consistent codes: a single-mode stationary code and a multi-mode time-dependent code. At a given beam current the cathode voltage used in the simulations is the maximum voltage which results in stable

operation with maximum computed power (see Fig. 24). The curve computed from the time-dependent multi-mode code shows the maximum output power found in stable operation. The code was operated with five modes; the operating mode $TE_{31,17}$ and the four next and over-next azimuthal neighbours $TE_{29,17}$, $TE_{30,17}$, $TE_{32,17}$ and $TE_{33,17}$. Stability was checked with the cathode voltage constant up to 200 nsec. For low beam current (< 33 A) the numerical results follow closely the experimental data and the difference in power is not more than 15%. For higher current (40 to 45 A) the difference grows to 25% and finally for beam current at 50 A it reaches 30% for the stationary code. For beam current up to 46 A the two codes predicted the same maximum output power at the same cathode voltage. No mode competition was found and the codes predicted the same output power. At beam current 50 or 52 A the time-dependent code predicted less output power in stable operation than the stationary code, due to competition from the azimuthal neighbours. When mode competition is predicted from the multi-mode code the difference from the experimental result is not significant; 219 and 46 kW in absolute values, respectively. At beam current less than 46 A the time-dependent code predicted no mode competition but the difference from the experimental result is considerable (1.33 MW computed and 0.93 MW measured). The reason is probably enhanced mode competition due to window reflections and the increased diffractive quality factor of the competing modes. The stability region of the $TE_{31,17}$ mode in the I_b - U_c plane is presented in Fig. 24.

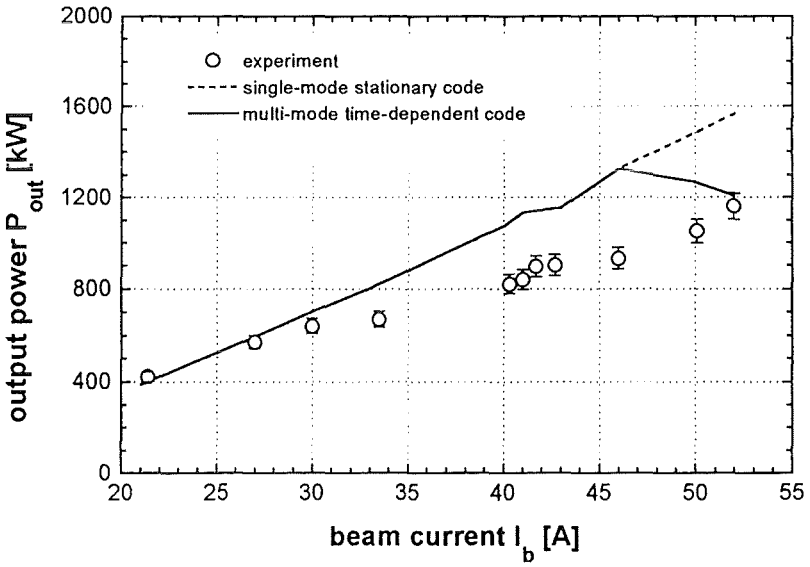

Fig. 23: Maximum output power in the operating $TE_{31,17}$ mode versus the beam current; theory and experiment.

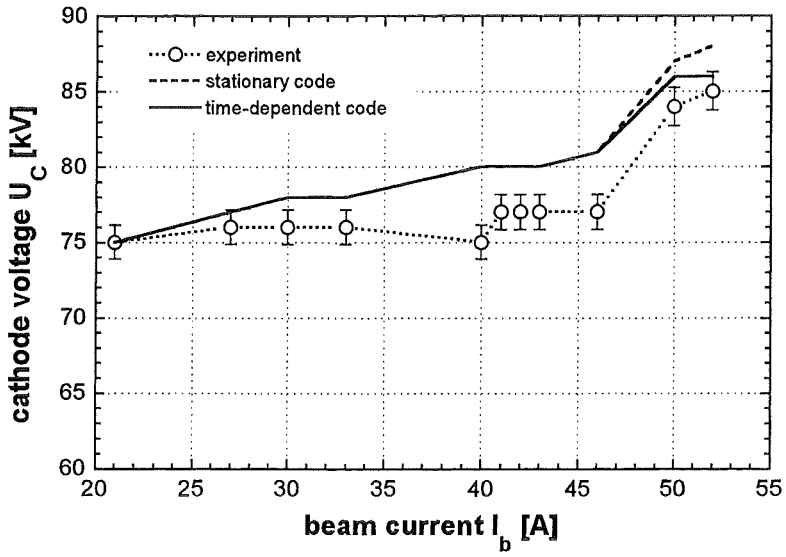

Fig. 24: Stability region of the operating $TE_{31,17}$ mode; theory and experiment.

The output power and the corresponding efficiency in different modes versus the cathode voltage are presented in Figs 25. The first gun-coil ES1 was energized. The cavity magnetic field is 6.55 T, the beam radius is at 9.62 mm, while the dependence of beam current and electron pitch angle on the cathode voltage is shown in Fig. 26. At cathode voltage 77 kV and beam current 40 A the electron pitch angle is equal to 1.0 and the rms value of the transverse electron velocity spread 7%, according to EGUN computations. Three frequencies were observed in the experiment at different ranges of cathode voltage; below 60 kV the tube was oscillating at 169.52 GHz in the $TE_{33,17}$ mode with maximum output power 0.39 MW ($\eta = 17.9\%$); in the voltage range from 62 to 68 kV monomode oscillations were observed at 167.27 GHz in $TE_{32,17}$ mode with maximum output power 0.57 MW ($\eta = 21.5\%$). The operating mode $TE_{31,17}$ was observed at 164.98 GHz in the cathode voltage range from 71 to 76.5 kV. The maximum power delivered in this mode was 0.90 MW at cathode voltage 76.5 kV and beam current 41.7 A with efficiency 28.1%. Between the different monomode stages multimode operation was observed. In Figs 25 open circles present monomode oscillations, while open circles with cross show multimoding. The curves represent the numerical results of the time-dependent multi-mode code. The maximum experimentally obtained output power in the $TE_{33,17}$ mode agrees well with the computed result, but the operating region of this mode extended experimentally to higher cathode voltages. This can be explained by the significantly increased diffractive quality factor of this mode due to window reflections. The change from the $TE_{32,17}$ to the $TE_{31,17}$ agrees well with the experiment and takes place close to 70 kV cathode voltage. The operating region of the $TE_{31,17}$ is considerably compressed in the experiment, possibly due to window reflections and beam instabilities at high cathode voltage (high beam α). In the experiment the operating mode lost oscillations at cathode voltage 76.5 kV with power 0.90 MW ($\eta = 28.1\%$), while the simulations predicted stable oscillations even at 80.5 kV with power 1.14 MW ($\eta = 34.8\%$).

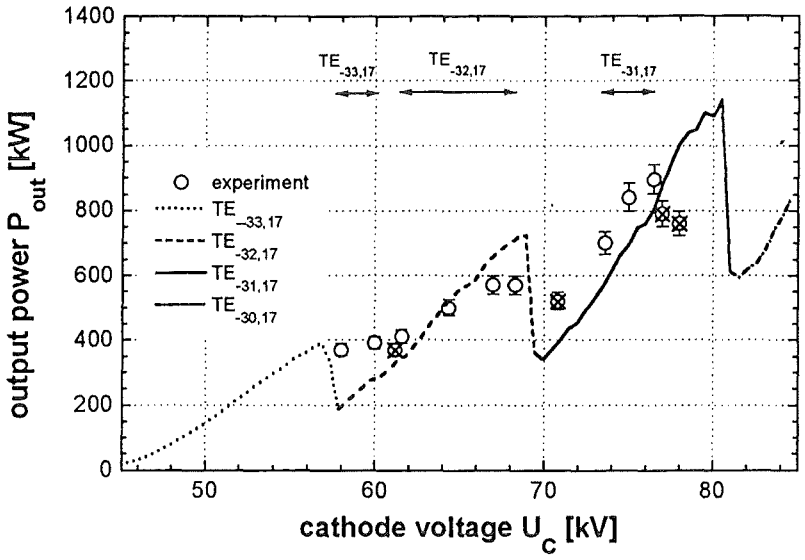

Fig. 25a: Output power in different modes versus the cathode voltage. ES1 gun-coil energized; $B_0 = 6.55$ T, $R_b = 9.62$ mm, $\delta\beta_{\perp,\mathrm{rms}} = 7\%$, and $\alpha = 1.0$ at $U_c = 77$ kV and $I_b = 40$ A. Crossed circles show multimoding.

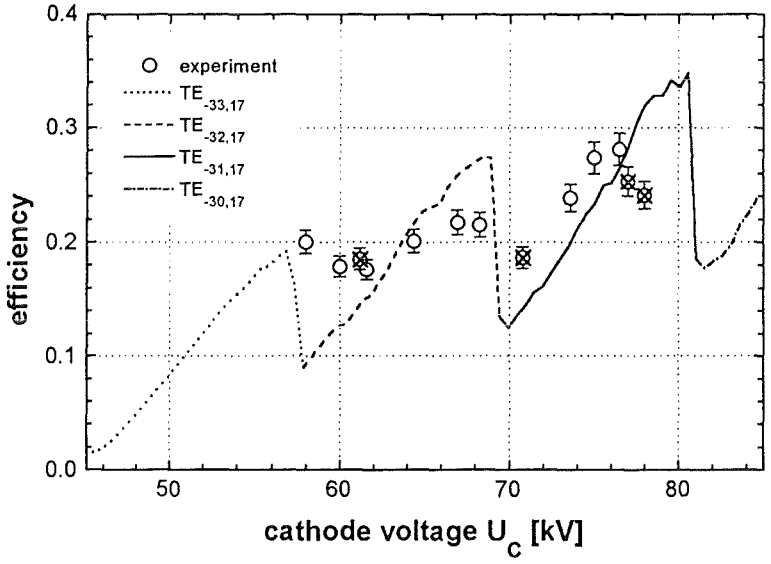

Fig. 25b: Total efficiency of different modes versus the cathode voltage. ES1 gun-coil energized; $B_0 = 6.55$ T, $R_b = 9.62$ mm, $\delta\beta_{\perp,\mathrm{rms}} = 7\%$, and $\alpha = 1.0$ at $U_c = 77$ kV and $I_b = 40$. Crossed circles show multimoding.

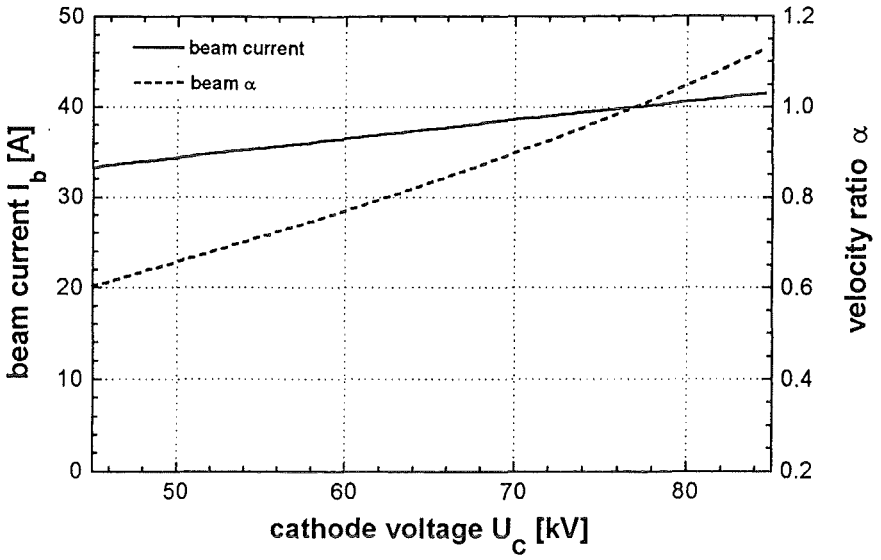

Fig. 26: Beam current and electron pitch angle versus the cathode voltage. ES1 gun-coil energized; $B_0 = 6.55$ T, $R_b = 9.62$ mm, $\alpha = 1.0$ at $U_c = 77$ kV and $I_b = 40$ A.

The main reason that prevented stable operation in the $TE_{31,17}$ mode at higher cathode voltage is the appearance of beam instabilities due to increased velocity spread. With increasing the cathode voltage the beam α increases, but the electron velocity spread increases as well. The same effects were observed trying to increase the beam current above 45 A. The beam was often unstable and the operation of the tube difficult. With the increase of the cavity beam radius (lower compression - lower beam α) the beam was more stable and vice versa. This is an additional sign for development of beam instabilities at regions of high beam α. For this reason the second gun-coil ES2 was operated instead of the ES1. This results in a lower beam α at higher cathode voltage and beam current. In Figs 27 the output power and total efficiency are presented versus the cathode voltage. The cavity magnetic field is 6.63 T, the beam radius 9.63 mm, while the dependence of beam current and electron pitch angle α on the cathode voltage is shown in Fig. 28. At 84 kV cathode voltage and 50 A beam current the beam α is equal to 0.84 and the rms electron velocity spread is 3.5%, according to EGUN computations.The beam was stable up to 50 A and even more. Experimentally only two frequencies were measured in monomode operation; 168.52 GHz ($TE_{33,17}$ mode) and 164.99 GHz ($TE_{31,17}$ mode). In an extended cathode voltage range (70 to 77 kV) it was observed multimoding of these two frequencies and the $TE_{32,17}$ mode at 167.27 GHz. The agreement between the numerical and experimental results of the operating $TE_{31,17}$ mode is almost perfect. Experimentally the mode found to oscillate up to 84.6 kV cathode voltage and 52 A current with output power 1.06 MW and efficiency 24.1%. Assuming 7% ohmic losses and 1.5 kV voltage depression, an electronic efficiency of 26.4% is computed. The beam α is 0.85 and the transverse electronic efficiency at 62.9%. Numerically the $TE_{31,17}$ mode was found to oscillate up to 86.7 kV with output power 1.19 MW and 27.1% total efficiency. It was not possible in the experiment to increase the cathode voltage more than 85 kV because of high - voltage

power supply limitations. In general, the operation of the tube with the gun-coil ES2 energized was very smooth and easy, because of the low beam α and the absence of any beam instabilities.

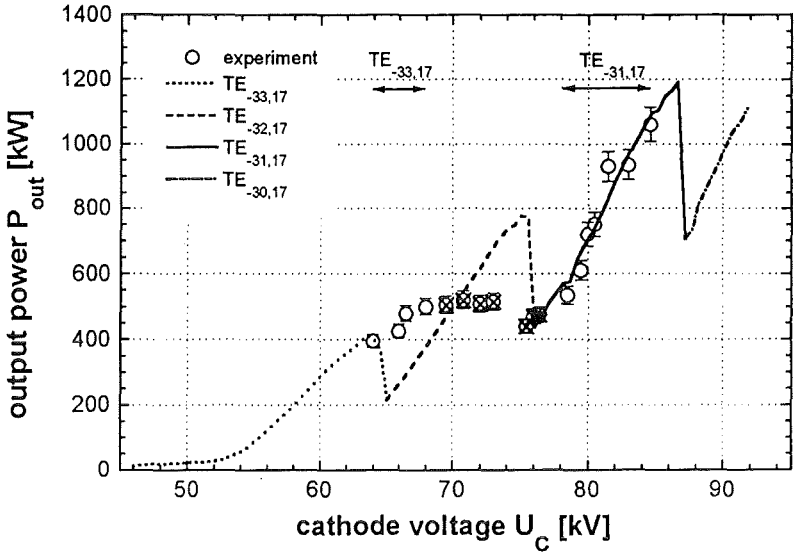

Fig. 27a: Output power in different modes versus the cathode voltage. ES2 gun-coil energized; $B_0 = 6.63$ T, $R_b = 9.63$ mm, $\delta\beta_{\perp,\mathrm{rms}} = 3.5\%$, and $\alpha = 0.84$ at $U_c = 84$ kV and $I_b = 50$ A. Crossed circles show multimoding.

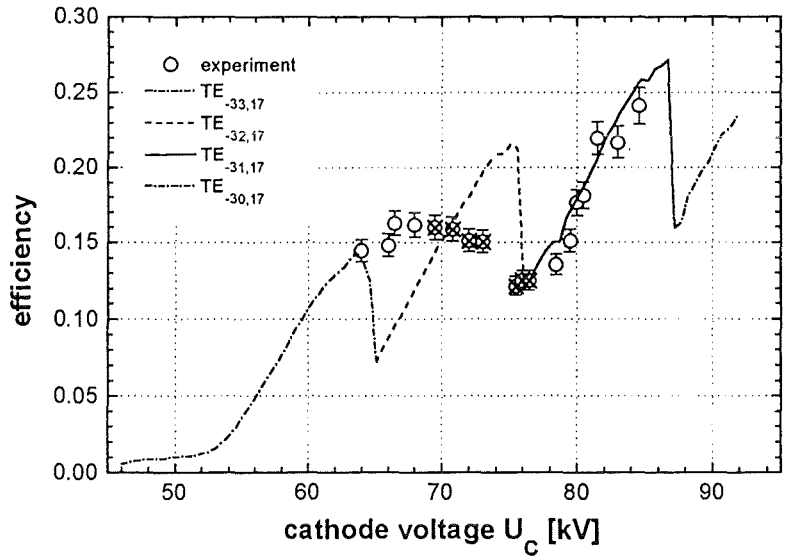

Fig. 27b: Total efficiency of different modes versus the cathode voltage. ES2 gun-coil energized; $B_0 = 6.63$ T, $R_b = 9.63$ mm, $\delta\beta_{\perp,\mathrm{rms}} = 3.5\%$, and $\alpha = 0.84$ at $U_c = 84$ kV and $I_b = 50$ A. Crossed circles show multimoding.

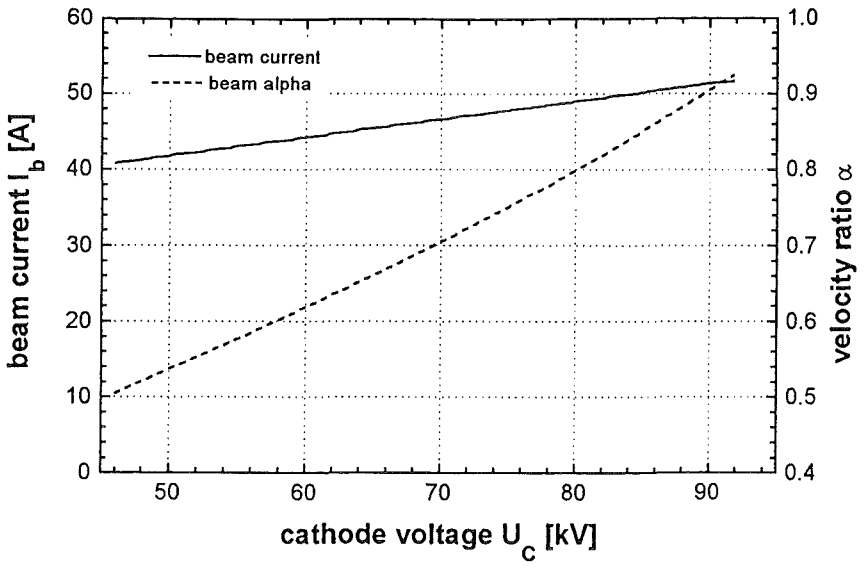

Fig. 28: Beam current and electron pitch angle versus the cathode voltage. ES2 gun-coil energized; $B_0 = 6.63$ T, $R_b = 9.63$ mm, $\alpha = 0.84$ at $U_c = 84$ kV and $I_b = 50$ A.

The maximum delivered output power in the operating $TE_{-31,17}$ mode was 1.17 MW and it was observed with the ES2 gun-coil energized at 6.63 T magnetic field, 9.63 mm beam radius, 86 kV cathode voltage and 51 A beam current. The corresponding total efficiency was 26.7%, the electronic efficiency 29.2% and the transverse electronic efficiency 68.6%. Similar operation was observed with the ES1 gun-coil energized (1.16 MW output power, 26.6% total efficiency, 6.62 T magnetic field, 9.55 mm beam radius, 84 kV cathode voltage and 52 A beam current), but the operation was very often unstable. The maximum efficiency was 28.2% with output power 0.90 MW and it was observed by energizing the ES1 gun-coil at 6.55 T magnetic field, 9.62 mm beam radius, 76 kV vathode voltage and 42 A beam current. The electronic efficiency is 30.9% and the corresponding transverse efficiency 62.8%. The tube was also operated at higher frequencies and the maximum power achieved is presented in Tab. 12. It is important to mention the megawatt level output power (1.02 MW) at 167.14 GHz frequency with efficiency 26.8%.

Tab. 12: Maximum output power delivered at different frequencies.

mode TE_{mn}	$TE_{31,17}$	$TE_{32,17}$	$TE_{33,17}$	$TE_{34,17}$
frequency f (GHz)	164.98	167.14	169.46	171.80
magnetic field B_0 (T)	6.63	6.62	6.62	6.62
beam radius R_b (mm)	9.63	9.70	9.75	9.82
cathode voltage U_c (kV)	86	76	70	57
beam current I_b (A)	51	50	50	46
output power P_{out} (MW)	1.17	1.02	0.63	0.35
total efficiency η_{tot} (%)	26.7	26.8	18.0	13.3

The far field pattern of the $TE_{31,17}$ mode generated in the gyrotron cavity has been measured using the set-up shown in Fig. 29. A nonlinear uptaper is connected after the rf output window of the tube to increase the diameter from 100 mm to 140 mm. A quartz glass plate is used to produce a standing-wave pattern from the rotating $TE_{31,17}$ mode and a teflon lens with 165 mm focal length focuses the radiation at a dielectric target plate. The far field pattern of the 165 GHz - $TE_{31,17}$ coaxial gyrotron output is shown in Fig. 30 where 62 minima and maxima are easily recognized.

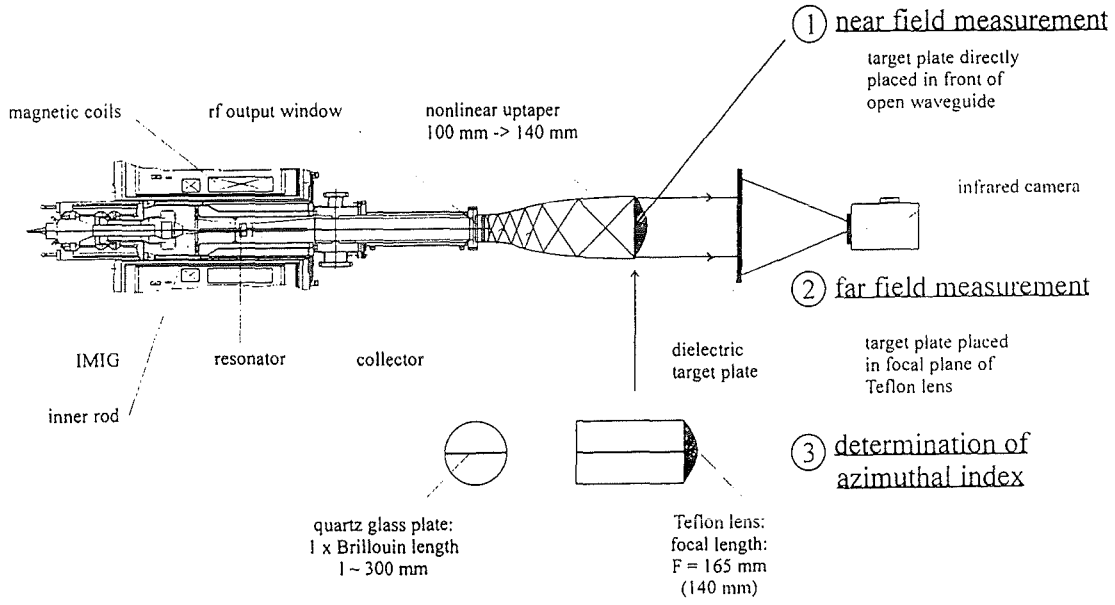

Fig. 29: Set-up for the field-pattern measurements of the 165 GHz - $TE_{31,17}$ coaxial gyrotron with axial output coupling.

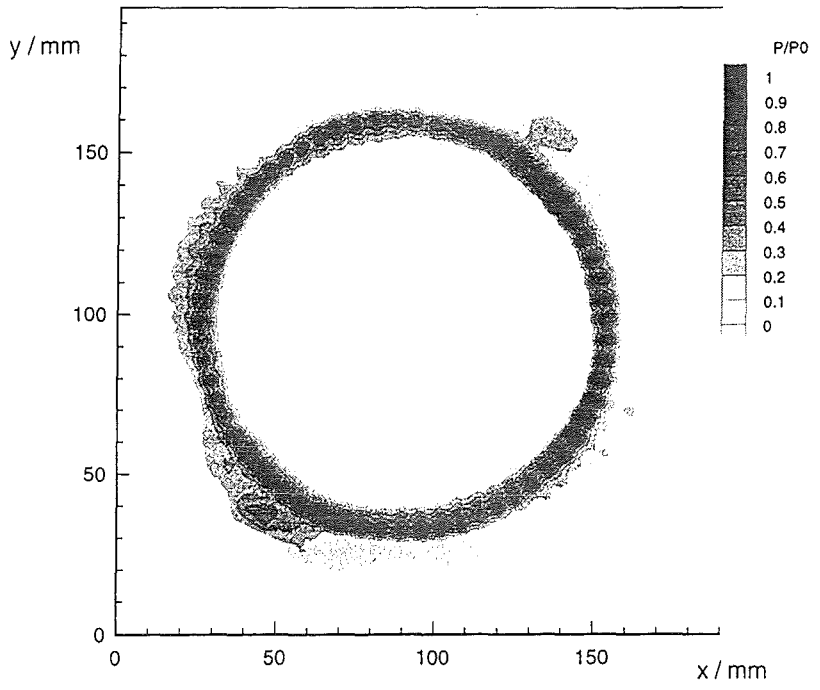

Fig. 30: Far field pattern of the 165 GHz - $TE_{31,17}$ coaxial gyrotron (quartz glass plate).

4. Subtask 4: Optimization and Design of a Q.O. Mode Converter System Compatible with the Coaxial Gyrotron Dual-Beam Output Concept for Operation with Two Output Windows.

Summary

The optimization and design of a quasi-optical (q.o.) mode converter system compatible with the constraints of a coaxial gyrotron dual beam output concept for operation with two output windows are presented. The two-step mode conversion schemes $TE_{-28,16}$ to $TE_{+76,2}$ to TEM_{00} at 140 GHz and $TE_{-31,17}$ to $TE_{+83,2}$ to TEM_{00} at 165 GHz have been investigated which both generate two narrowly-directed (60° at the launcher) output wave beams. The conversion of the co-rotating cavity mode to its degenerate counter-rotating WGM is achieved in a rippled-wall waveguide mode converter. The q.o. WGM to TEM_{00} mode converters employ improved dual-beam dimple-type launchers. High conversion efficiencies are expected (94% and 92%, respectively).

4.1 Introduction

Owing to the power limit of gyrotron rf windows, the mm-wave output power of a 2 MW coaxial cavity gyrotron must be split into two linearly polarized wave beams and coupled out radially through two 1 MW windows. Beam splitting can be performed either by a quasi-optical 3 dB splitter (e.g. special non-quadratic phase correcting mirror or a diffraction grating, Fig. 31), or by a dual-beam launcher of a q.o. mode converter (Fig. 32).

The advantage of the second solution is that an improved dimple-type launcher generating two output beams is much shorter than a single-beam launcher. If one employs, as in conventional cylindrical cavity gyrotrons, a q.o. mode converter for the operating volume mode of the cavity, the dimensions of the mirror system are excessively large for a dual beam output since the azimuthal angle of divergence φ of the radiation is quite large, e.g. $\varphi = 2\arccos(m / \chi_{mp}) = 142.62°$ for the $TE_{28,16}$ mode (Fig. 33a).

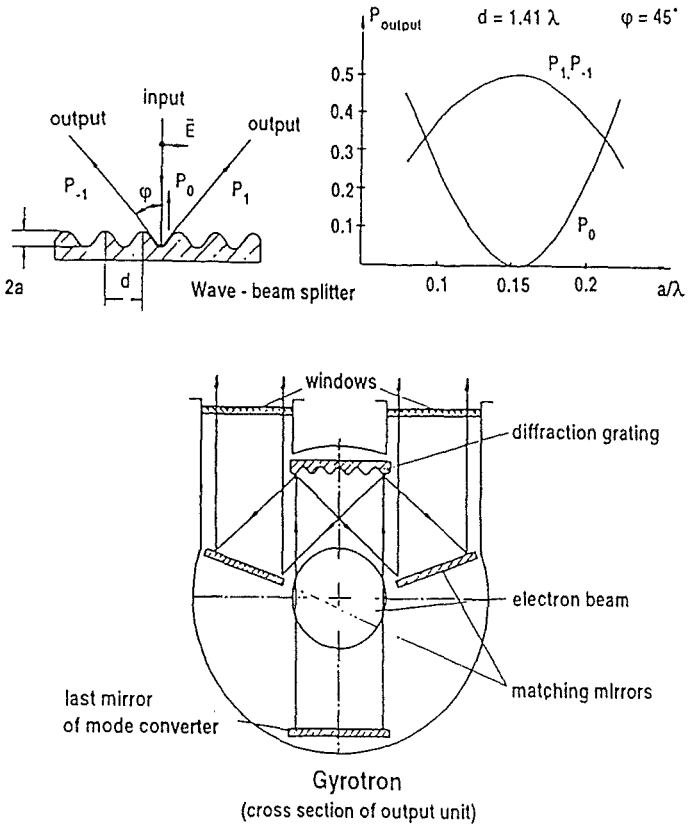

Fig. 31: Dual-beam rf output using a wave beam splitter (IAP Nizhny Novgorod).

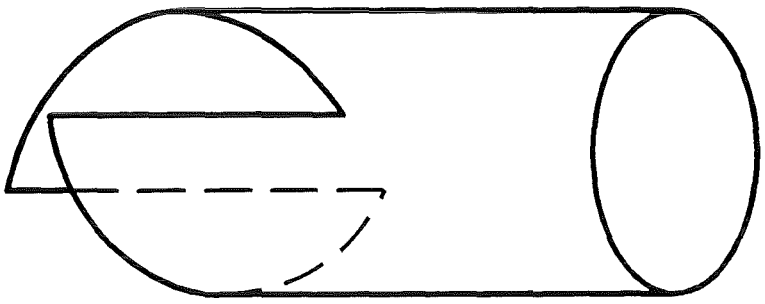

Fig. 32: Dual-beam launcher of a q.o. mode converter.

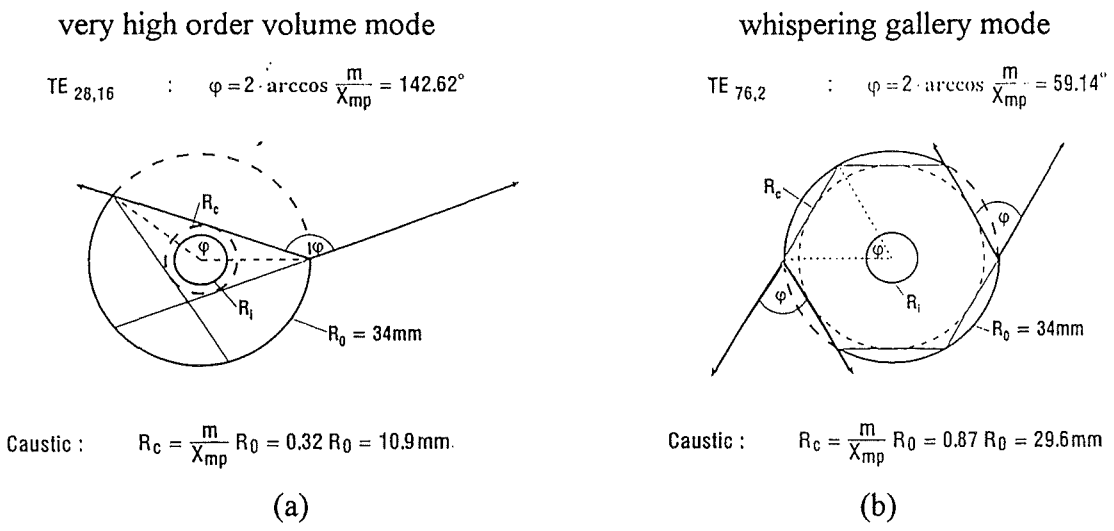

Fig. 33: Comparison of a volume mode with a WGM for use in a double-beam q.o. mode converter in a coaxial gyrotron.

This is not the case for a high-order whispering gallery mode (WGM) of the type $TE_{m,2}$ since here the representing rays from a caustic located closer at the waveguide wall, e.g. $\varphi \approx 2\arccos(m/\chi_{mp}) = 59.14°$ for the $TE_{76,2}$ mode (Fig. 33b) so that a double-cut q.o. launcher can generate two diametrically opposed narrowly-directed output wave beams.

The actual design of a q.o. mode converter system compatible with the constraints of a coaxial gyrotron dual beam output concept for operation with two output windows employs the two-step mode conversion schemes (w.g. = waveguide):

	w.g.		q.o.		
$TE_{-28,16}$	$(\chi_{mp} = 87.36)$	$\rightarrow$ $TE_{+76,2}$	$(\chi_{mp} = 87.38)$	$\rightarrow$ TEM_{00} at 140GHz	(1)
$TE_{-31,17}$	$(\chi_{mp} = 94.62)$	$\rightarrow$ $TE_{+83,2}$	$(\chi_{mp} = 94.69)$	$\rightarrow$ TEM_{00} at 165GHz	(2)

which both generate two narrowly directed (60° at the launcher) output wave beams. The q.o. mode converters are using improved dimple-type launchers. The WGMs $TE_{76,2}$ and $TE_{83,2}$ are degenerate to the operating volume modes in the gyrotron cavities, $TE_{28,16}$ and $TE_{31,17}$, respectively.

4.2 In-Waveguide Mode Conversion: Cavity Volume Mode to WGM

The conversion of the co-rotating cavity mode to its degenerate counter-rotating WGM is achieved by the introduction of longitudinal corrugations in the output taper (1.5°) of the gyrotron cavity according to the formula:

$$R_c(z) = R_{c,0}(z) + \rho\cos(\Delta m\phi)$$

where $R_{c,0}(z)$ is the mean radius of the tapered waveguide wall, ρ is the amplitude of corrugations and Δm = 104 and Δm = 114 for the mode conversion sequence (1) and (2), respectively. The parameters of the two optimized converters are summarized in Tab. 13.

Tab. 13: Parameters of two optimized waveguide mode converters.

	140 GHz (1)	165 GHz (2)
converter length (mm)	78	64
input radius (mm)	30.20	27.77
mean output radius (mm)	32.25	29.45
corrugation amplitude (mm)	0.057	0.052
ohmic losses (%) (enhancement factor: 1.5)	1.7	1.8
mode purity (%)	99	99

The corrugation depth is tapered at the input and output of the converters for a length of 12 mm at 140 GHz and 10 mm at 165 GHz. Conversion of the co-rotating cavity mode to the counter-rotating WGM and not to the co-rotating WGM has the advantage that the coupling coefficient is larger and coupling to unwanted modes is considerably reduced, since the modes $TE_{-132,1}$ and $TM_{-132,1}$ in converter (1) and $TE_{-145,1}$ and $TM_{-145,1}$ in converter (2) are below cutoff. Only the modes $TE_{+76,1}$, $TE_{+76,2}$ and $TE_{+76,3}$ (cutoff radius at 140 GHz = 31.8 mm) and $TE_{+83,1}$, $TE_{+83,2}$ and $TE_{+83,3}$ (cutoff radius at 165 GHz = 29.14 mm) can propagate in converter (1) and (2), respectively.

Figures 34, 35 and 36 show the calculated relative power, ohmic losses and the ohmic wall loading (for ideal cooper) along the $TE_{-28,16}$ - to - $TE_{+76,2}$ and the $TE_{-31,17}$ - to - $TE_{+83,2}$ mode converters. The calculations have been done in two-mode approximation. The numerical integration of the corresponding coupled-wave equations for all propagating modes showed that the mode purity is better than 99%.

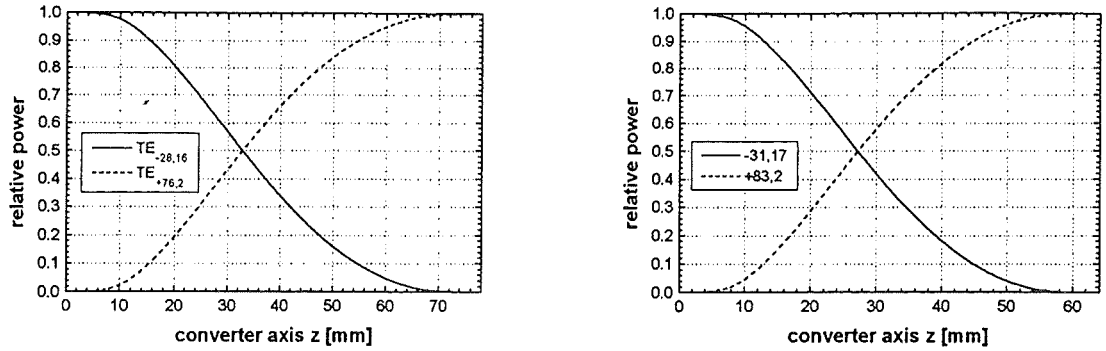

(a) (b)

Fig. 34: Relative power along the converter (a): $TE_{-28,16}$ - to - $TE_{+76,2}$ at 140 GHz and (b): $TE_{-31,17}$ - to - $TE_{+83,2}$ at 165 GHz.

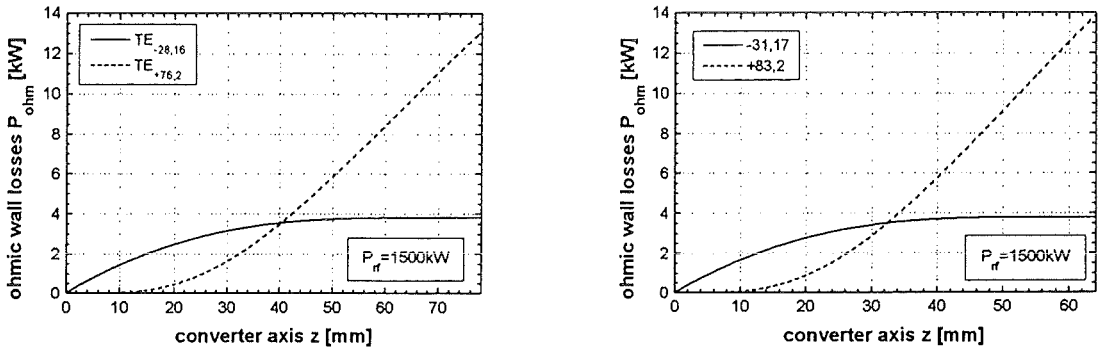

(a) (b)

Fig. 35: Ohmic losses along the converter (a): $TE_{-28,16}$ - to - $TE_{+76,2}$ at 140 GHz and (b): $TE_{-31,17}$ - to - $TE_{+83,2}$ at 165 GHz.

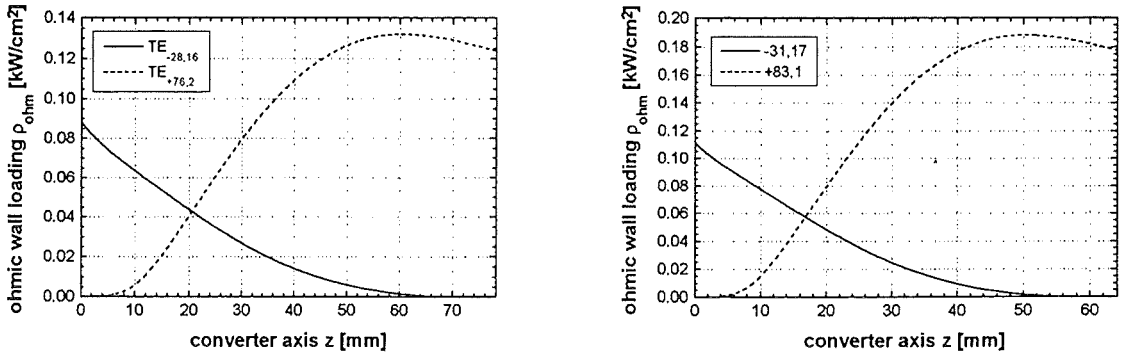

(a) (b)

Fig. 36: Ohmic wall loading along the converter (a): $TE_{-28,16}$ - to - $TE_{+76,2}$ at 140 GHz and (b): $TE_{-31,17}$ - to - $TE_{+83,2}$ at 165 GHz.

4.3 Quasi-Optical Mode Conversion: WGM to TEM_{00}

The q.o. WGM to TEM_{00} converters will use improved dual-beam dimple-type launchers with $\Delta m_1 = 2$ and $\Delta m_2 = 6$ perturbations for longitudinal and azimuthal bunching of the two mm-wave beams. The parameters of the two advanced launchers are given in Tab. 14.

Tab. 14: Parameters of two dimple-type dual-beam launchers.

	140 GHz (1)	165 GHz (2)
launcher length (mm)	228	258
average diameter (mm)	68.3	62.8
Brillouin angle (°)	60.7	60.7
vertical beam radius (mm)	9.8	13.9
horizontal beam radius (mm)	12.0	17.0
ohmic losses (%)	4.6	5.9
efficiency (%)	95	93

Figure 37 shows the theoretical intensity contour map of an advanced double beam launcher for the $TE_{76,2}$ mode at 140 GHz.

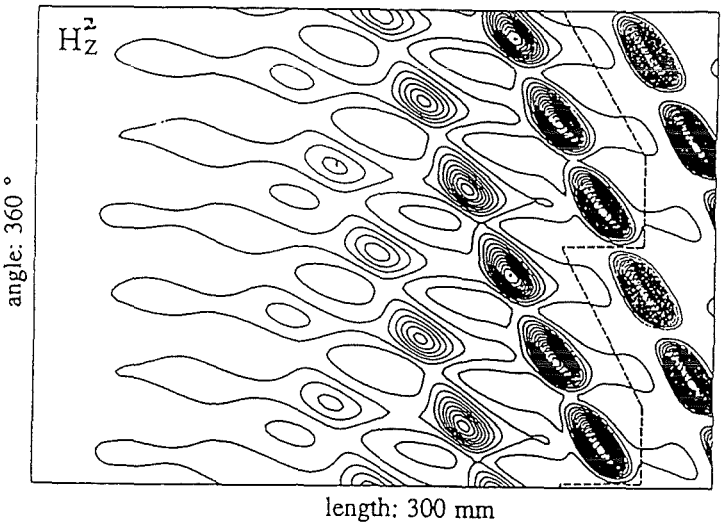

Fig. 37: Theoretical intensity contour map of a dimple-type double-beam launcher for the $TE_{76,2}$ mode at 140 GHz.

The radii w of the two output beams on the two fused silica windows (100 mm diameter) were selected to be 26 mm. The two optimized phase-correcting and beam-shaping output mirrors for one beam are described by the following gyrotron coordinates ($z = 0$, center of cavity, see Fig. 38)

Lower mirror

	x (mm)	y (mm)	z (mm)
center:	61.47	29.71	432.55
corners:	55.11	2.92	454.89
	54.83	3.09	432.55
	60.94	68.68	461.18
	60.65	68.51	420.15

Upper mirror

	x (mm)	y (mm)	z (mm)
center:	-156.91	85.47	559.23
corners:	-131.07	197.55	605.28
	-180.72	136.79	448.53
	-135.27	34.21	669.94
	-184.93	-26.55	513.19

The coordinates of the two mirrors for the second output beam are symmetric to these values with respect to the gyrotron axis.

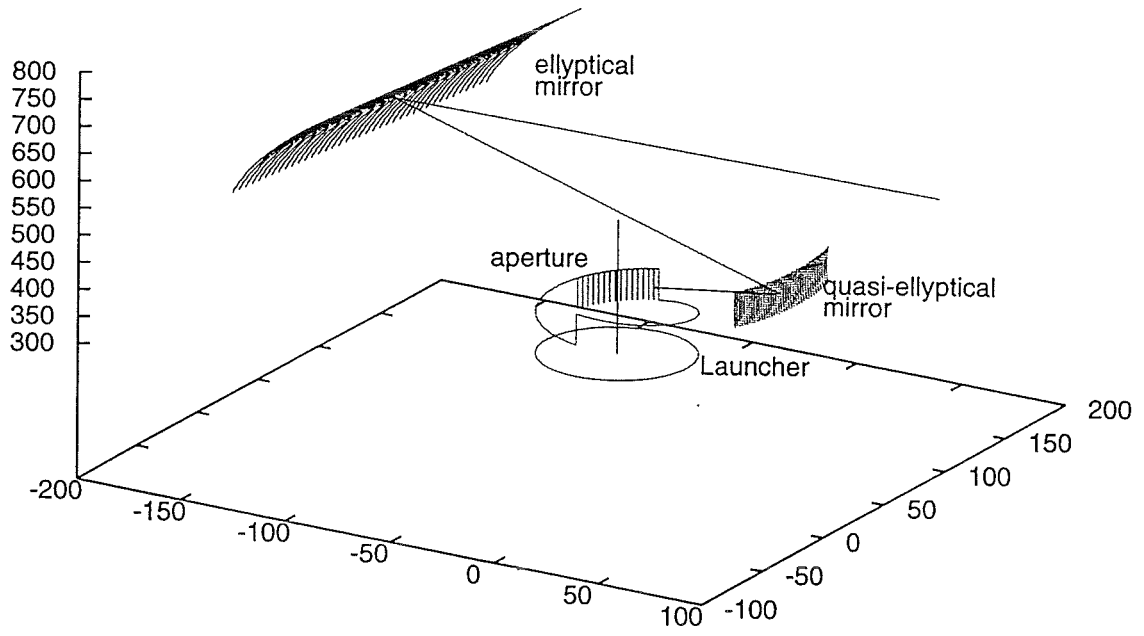

Fig. 38: Mirror system for double-beam q.o. mode converter for a 140 GHz coaxial cavity gyrotron with two output windows (system for only one beam is shown).

4.4 Backscattering Analysis of Dual-Beam Launchers

The backscattering effects due to diffraction of the incident high-order WGM by the helical and straight edges of the dual-beam launcher have been calculated using the method of equivalent currents [10]. Because of the complex shape of the launcher, the incident mode n is scattered back into all modes which can propagate. Modes j which fulfill the resonance condition

$$2\pi (m_n - m_j) + kL(\cos\psi_n + \cos\psi_j) \approx 0$$

are excited strongly. Here L is the length of the straight cuts and $\psi = \chi_{mp} / kR$, where k is the free-space wavenumber and R is the launcher radius. For resonable values of the Brillouin angle ψ_n this condition can be satisfied only for high-order WGMs. The total reflected power of the incident $TE_{76,2}$ mode scattered from a double-cut launcher at 140 GHz is plotted in Fig. 39. As can be seen the total reflected power can be reduced by choosing a proper Brillouin angle (in our case $\psi_n = 60.7°$).

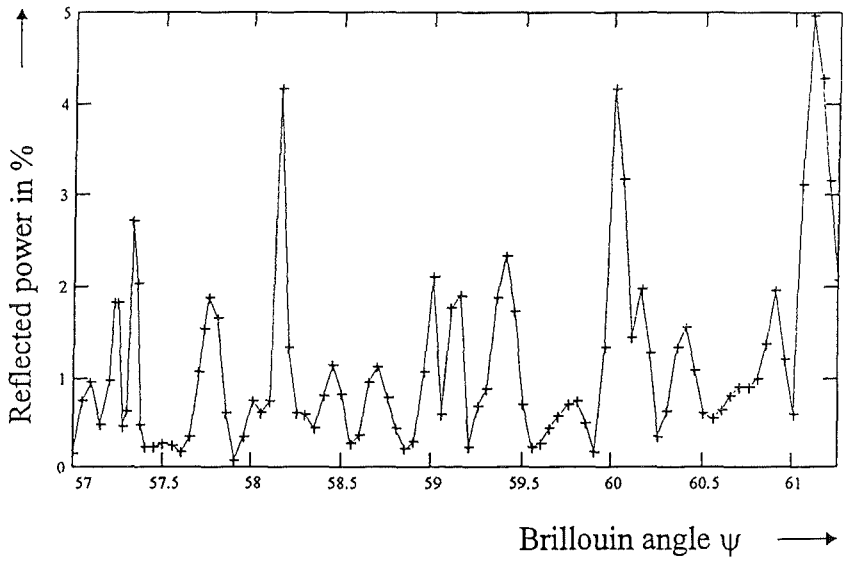

Fig. 39: Total reflected power of a double cut launcher versus Brillouin angle ψ.

4.5 Low-Power Tests of the Mode-Converter Sequence at 140 GHz

Based on previous designs consisting of a coaxial cavity with a perforated wall and a specific mirror (Fig. 40) [11], [12] we have designed and manufactured a $TE_{+76,2}$-mode generator in order to do cold tests on the 140 GHz mode converter for the $TE_{28,16}$ coaxial cavity gyrotron. Figure 41 shows the measured field pattern at the mode generator output. A rectangular D-band waveguide was used for mm-wave detection, so only one polarization was measured each time.

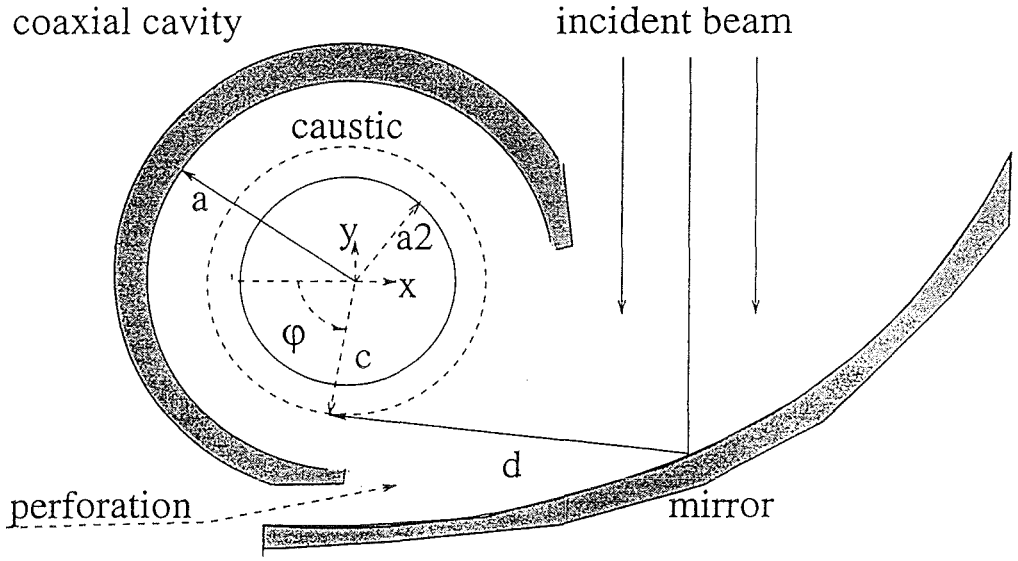

Fig. 40: Schematic of $TE_{+76,2}$ mode generator.

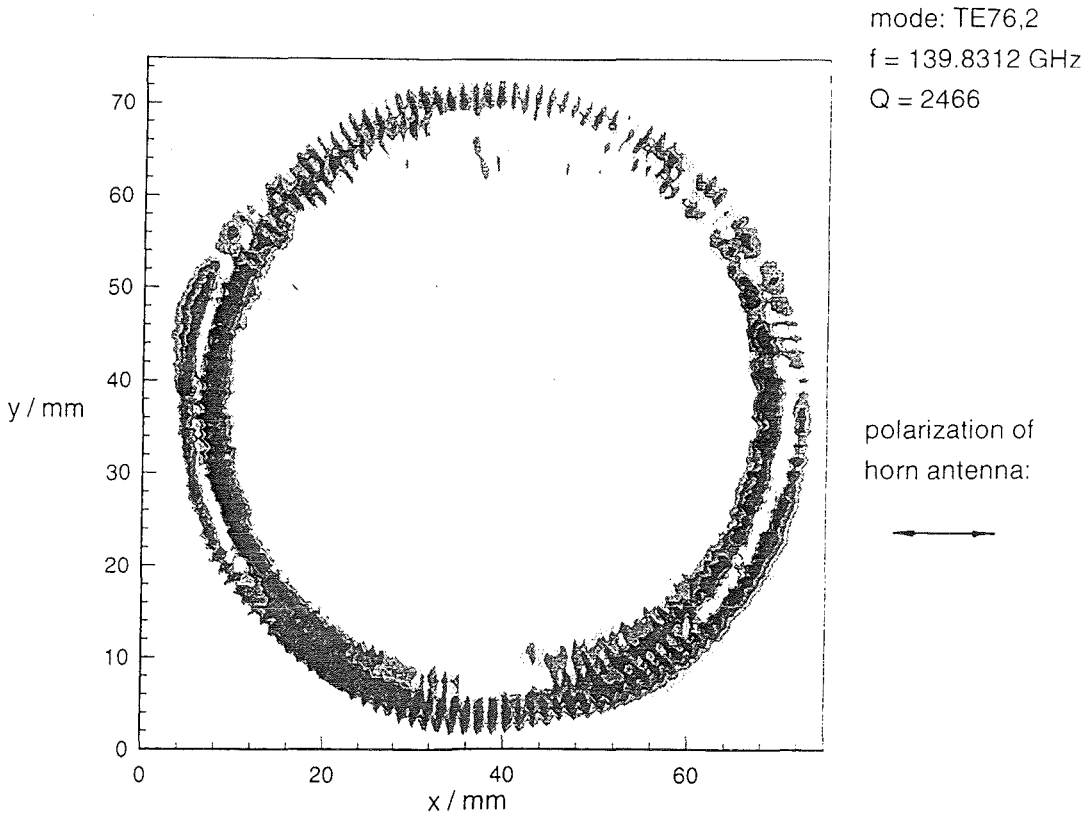

Fig. 41: Pattern of rotating $TE_{76,2}$ mode at 140 GHz with approximately 0.5% of counter rotating mode

4.6 Extrapolation to CW Operation - Internal Losses

In order to discuss the cw capability of a 2 MW coaxial gyrotron the calculated losses in different parts of the tube are summarized in Tab. 15 and compared with those of a 1 MW conventional cylindrical cavity gyrotron. In the case of the coaxial gyrotron we consider two versions:

(1) The cavity mode $TE_{28,16}$ is converted to a Gaussian output (one beam, e.g. LNe-cooled 2 MW sapphire window)

(2) The cavity mode $TE_{28,16}$ is converted to the whispering gallery mode $TE_{76,2}$ for dual-beam Gaussian output through two 1 MW windows.

The absolute losses in the coaxial gyrotron are larger, mostly due to the higher unit power, but the power densities are lower, so that no principal cooling problems should arise. In order to bring the stray radiation partially out of the tubes, the inner surfaces of coaxial gyrotrons must have a high reflectivity (copper, glidcop, copper plated stainless steel).

Tab. 15: Calculated losses in different parts of the gyrotron for different cases.

Component losses	Conventional 1 MW gyrotron	Coaxial 2 MW gyrotron	Coaxial 2 MW gyrotron (2)
cavity	4 %	2 % (1.8 % outer wall,	2 % 0.2 % inner rod)
up-taper	1.0 %	1.3 %	0.5 %
inner waveguide mode converter	-	-	1.8 %
q.o. converter - launcher - mirrors	1.0 %	1.0 %	4.6 %
(a) ohmic	0.4 %	0.6 %	0.6 %
(b) diffraction	3.0 %	5.0 %	4.0 %
stray radiation			
Total losses (%)	9.4 %	9.9 %	13.5 %
Total losses (kW)	95 kW	198 kW	270 kW
Stray radiation	30 kW	100 kW	80 kW

4.7 Disadvantages and Alternative Solutions

The disadvantages of the presented approach of the power extraction system are the relatively high ohmic losses of the WGM in the dual-beam launcher and that it is not probable to find more than one of these pairs of degenerate modes in a given design, so for stepwise frequency tunable gyrotrons other output structures are required.

The following alternative solutions of the power extraction system are possible:

(1) Usage of a q.o. launcher with tapered helical impedance corrugations which generate the hybrid modes $EH_{76,2}$ at 140 GHz and $EH_{83,2}$ at 165 GHz, modes that have ohmic attenuation in the launcher comparable to that of the cavity working modes (approx. 1%). The problem in this case is the complicated manufacturing ofthe launcher.

(2) Direct usage of the cavity working mode $TE_{28,16}$ at 140 GHz and $TE_{31,17}$ at 165 GHz in a dimple launcher with $\Delta m_1 = 1$ and $\Delta m_2 = 5$ perturbations in order to create two output beams. But in this case the two beams emerge at different z-positions and have an angle of about 140°.

Solution (2) provides the possibility of stepwise frequency tuning.

References

[1] Vlasov, S. N., Zagryadskaya, L. I., and Orlova, I. M., 1976, Open coaxial resonators for gyrotrons. *Radio Engineering and Electronic Physics*, **21**, 96-102.

[2] Iatrou, C. T., Kern, S., and Pavelyev, A. B., 1996, Coaxial cavities with corrugated inner conductor for gyrotrons. *IEEE Transactions on Microwave Theory and Techniques*, **41**, 56-64.

[3] Barroso, J. J., and Correa, R. A., 1991, Coaxial resonator for a megawatt, 280 GHz gyrotron. *International Journal of Infrared and Millimeter Waves*, **12**, 717-728.

[4] Lygin, V. K., Manuilov, V. N., Kuftin, A. N., Pavelyev, A. B., Piosczyk, B., 1995, Inverse magnetron injection gun for a 1.5 MW, 140 GHz gyrotron. *International Journal of Electronics*, **79**, 227-235.

[5] Flyagin, V. A., Khishnyak, V. I., Manuilov, V. N., Pavelyev, A. B., Pavelyev, V. G., Piosczyk, B., Dammertz, G., Höchtl, O., Iatrou, C. T., Kern, S., Nickel, H.-U., Thumm, M., Wien, A., and Dumbrajs, O., 1994, Development of a 1.5 MW coaxial gyrotron at 140 GHz. *19th International Conference on Infrared and Millimeter Waves*, Conference Digest **JSAP 941228**, 75-76, Sendai, Japan.

[6] Piosczyk, B., Braz, O., Dammertz, G., Iatrou, C. T., Kern, S., Möbius, A., Thumm, M., Wien, A., Zhang, S. C., Flyagin, V. A., Khishnyak, V. I., Kuftin, A. N., Manuilov, V. N., Pavelyev, A. B., Pavelyev, V. G., Postnikova, A. N., and Zapevalov, V. E., 1995, Development of a 1.5 MW, 140 GHz Coaxial Gyrotron. *20th International Conference on Infrared and Millimeter Waves*, 423-424, Lake Buena Vista (Orlando), Florida, USA.

[7] Kern, S., Iatrou, C. T., and Thumm, M., 1995, Investigations on mode stability in coaxial gyrotrons. *20th International Conference on Infrared and Millimeter Waves*, 429-430, Lake Buena Vista (Orlando), Florida, USA.

[8] Iatrou, C. T., Braz, O., Dammertz, G., Kern, S., Piosczyk, B., Thumm, M., Wien, A., and Zhang, S. C., 1995, Development of a 1.5 MW coaxial gyrotron at 165 GHz. *20th International Conference on Infrared and Millimeter Waves*, 415-416, Lake Buena Vista (Orlando), Florida, USA.

[9] Iatrou, C. T., 1996, Mode selective properties of coaxial resonators. *IEEE Transactions on Plasma Science*, **24**(3).

[10] Wien, A., and Thumm, M., 1995, Backscattering analysis of shaped-end radiators of quasi-optical mode converters using the method of equivalent currents. *International Conference on Infrared and Millimeter Waves*, 469-470, Lake Buena Vista (Orlando), Florida, USA.

[11] Braz, O., Kern, S., Losert, M., Möbius, A., Pereyaslavets, M., and Thumm, M., 1995, Improvements of mode converters for low power excitation of gyrotron-type modes. *International Conference on Infrared and Millimeter Waves*, 471-472, Lake Buena Vista (Orlando), Florida, USA.

[12] Pereyaslavets, M., Braz, O., Kern, S., Losert, M., Möbius, A., and Thumm, M., 1996, Improvements of mode converters for low power excitation of gyrotron-type modes. *International Journal of Electronics*, accepted for publication.